CATÓLICA
FACULTY OF BIOTECHNOLOGY

PORTO

Multiple Sclerosis Lesion Segmentation in 2D T2-FLAIR Brain Magnetic Resonance Imaging

By

Vanessa Sofia Fernandes Ferreira

March 2024

CATÓLICA
FACULTY OF BIOTECHNOLOGY

PORTO

Multiple Sclerosis Lesion Segmentation in 2D T2-FLAIR Brain Magnetic Resonance Imaging

Dissertation submitted to the School of Biotechnology of the Portuguese Catholic University for the degree of Master of Science degree in Biomedical Engineering

By Vanessa Sofia Fernandes Ferreira

Supervisor: Professor António César da Silva Ferreira

March 2024

Abstract

This study aims to address the gap in automatic segmentation of Multiple Sclerosis lesions within 2D T2-FLAIR magnetic resonance imaging. The project was developed using a small basis dataset available on the Mendeley website, consisting of original images and corresponding segmentations executed by professional radiologists and neurologists.

Brain tissue extraction and data augmentation techniques were used to address the challenge posed by the lack of prior documentation, representing a significant advancement in preprocessing steps for this particular MRI modality.

During the brain extraction procedure, FSL from Oxford University was employed, namely BET (brain extraction tool), which was originally created for T1 modality images. This required necessary additional preprocessing of image pixels to resemble T1 images, including contrast adjustment. To ensure that image augmentation is well performed on both original image and segmentation, the transformers package from the Python environment was used. The augmentation consisted of simple procedures such as rotations, flips and noise addition with Gaussian blur.

The investigation has successfully developed and validated an automatic segmentation model for T2-FLAIR MRI images. The model achieved a remarkable Dice coefficient of almost 0.6 in a transformer architecture with 12 layers and attention heads, indicating substantial agreement with ground truth annotations.

Despite using a relatively small dataset, the results demonstrate the feasibility of the approach in clinical settings. The performance is commendable for its initial scope. However, to improve the accuracy and generalizability of the model, further data enrichment is necessary.

The success in extracting brain tissue and augmenting data, along with the encouraging segmentation outcomes, demonstrates the potential for more comprehensive studies. Future efforts should focus on expanding the dataset and refining the model to enhance the diagnostic and monitoring capabilities of Magnetic Resonance Imaging in Multiple Sclerosis management. This study presents a new approach to medical image processing and sets a fundamental precedent for future investigations into the automated segmentation of Multiple Sclerosis lesions in T2-FLAIR modality.

Keywords: Multiple Sclerosis, MRI, Automatic Segmentation, Machine Learning

Resumo

Este estudo tem como objetivo colmatar a lacuna na segmentação automática de lesões de Esclerose Múltipla em imagens de ressonância magnética (RM) 2D T2-FLAIR. O projeto foi desenvolvido usando um pequeno conjunto de dados de base disponível no site Mendeley, consistindo em imagens originais e segmentações correspondentes executadas por radiologistas e neurologistas profissionais.

As técnicas de extração de tecido cerebral e de aumento de dados foram utilizadas para responder ao desafio colocado pela falta de documentação prévia, representando um avanço significativo nos passos de pré-processamento para esta modalidade particular de RM.

Durante o procedimento de extração do cérebro, foi utilizada a FSL da Universidade de Oxford, nomeadamente a BET (ferramenta de extração do cérebro), que foi originalmente criada para imagens da modalidade T1. Isto exigiu um pré-processamento adicional dos pixéis da imagem para se assemelharem às imagens T1, incluindo o ajuste do contraste. Para garantir que o aumento da imagem é bem executado tanto na imagem original como na segmentação, foi utilizado a package *transformers* do ambiente Python. O aumento consistiu em procedimentos simples, como rotações, inversões e adição de ruído com desfocagem gaussiana.

A investigação desenvolveu e validou com êxito um modelo de segmentação automática para imagens de RM T2-FLAIR. O modelo alcançou um coeficiente Dice notável de quase 0,6 numa arquitetura de transformador com 12 camadas e cabeças de atenção, indicando uma concordância substancial com as anotações da verdade terrestre.

Apesar de utilizar um conjunto de dados relativamente pequeno, os resultados demonstram a viabilidade da abordagem em contextos clínicos. O desempenho é louvável para o seu âmbito inicial. No entanto, para melhorar a exatidão e a generalização do modelo, é necessário um maior enriquecimento dos dados.

O sucesso na extração de tecido cerebral e no aumento de dados, juntamente com os resultados encorajadores da segmentação, demonstra o potencial para estudos mais abrangentes. Os esforços futuros devem centrar-se na expansão do conjunto de dados e no aperfeiçoamento do modelo para melhorar as capacidades de diagnóstico e monitorização da Ressonância Magnética na gestão da Esclerose Múltipla. Este estudo

apresenta uma nova abordagem ao processamento de imagens médicas e estabelece um precedente fundamental para futuras investigações sobre a segmentação automática de lesões de Esclerose Múltipla na modalidade T2-FLAIR.

Palavras-chave: Esclerose Múltipla, RM, Segmentação Automática, Aprendizado de Máquina

Acknowledgements

First and foremost, I wish to express my deepest gratitude to my supervisor, Professor António César Ferreira, for their unwavering support and guidance throughout the course of this research. Your expertise and insight have been invaluable, not only to this thesis but also to my growth as a scholar. Your patience and dedication to excellence have profoundly shaped my journey through this academic endeavor.

I would also like to extend a heartfelt thanks to my mother, whose love and encouragement have been the bedrock of my perseverance. You have instilled in me the values of hard work and dedication, and your belief in my potential has been a constant source of strength. Your sacrifices have not gone unnoticed, and this achievement is as much yours as it is mine.

To my family, who have provided me with endless support and understanding, I am truly grateful. Your constant encouragement and faith in me, even when the goal seemed distant, have been sources of motivation that kept me focused and determined. I am blessed to have a family whose support is unwavering and who has celebrated each step of this journey with me.

A special acknowledgment goes out to my best friend, Rita, whose companionship and unwavering faith in my abilities have been a cornerstone of my personal and academic life. Your presence, optimism and help, even on the most challenging days, have brought light into the process and have reminded me of the joy in our shared moments of triumph.

I would also like to extend my sincere appreciation to Rafael for being a remarkable friend and all conversations and perspectives that enriched my life in more ways than I can count.

Every one of you has contributed to making this milestone possible, and for that, I am eternally grateful.

Table of Contents

List Of Abbreviations

- ANAs - Antinuclear Antibodies
- ANN - Artificital Neural Network
- BBB – Blood Brain Barrier
- BET – Brain Extraction Tool
- CIS - Clinical Isolated Syndrome
- CNN - Convolutional Neural Network
- CNS - Central Nervous System
- CSF - Cerebrospinal Fluid
- CT – Computed Tomography
- DMTs - Disease-modifying Therapies
- DSC - Dice Similarity Coefficient
- EDSS - Extended Disability Status Scale
- EPT - Electrical Properties Tomography
- FLAIR - Fluid-Attenuated Inversion Recovery
- GM - Gray Matter
- IoU - Intersection-over-Union
- MAE - Mean Absolute Erro
- MRI – Magnetic Resonance Imaging
- MS – Multiple Sclerosis
- MSE - Mean Squared Error
- PPMS - Primary Progressive Multiple Sclerosis
- ReLU - Rectified Linear Unit
- RF - Radiofrequency
- RRMS - Relapsing-Remitting Multiple Sclerosis
- SPMS - Secondary Progressive Multiple Sclerosis
- WM - White Matter
- ZTE - Zero Echo-time

Figure Index

Table Index

Equation Index

1. Introduction

This report presents the final results of a Master's Thesis to fulfill the of Master of Science degree in Biomedical Engineering performed at *Escola Superior de Biotecnologia of the Universidade Católica Portuguesa*. This chapter provides a short background and outlines the purpose of this work.

1.1.Contextualization

Multiple Sclerosis (MS) is the most common autoimmune-mediated disease in the world, according to the National Institute of Neurological Disorders and Stroke in the United States of America. It is characterized by chronic inflammation state along the Central Nervous System, which can lead to a wide range of cognitive and physical disabilities.

MS is a disease that typically affects young adults, with onset occurring typically between the ages of 20 and 40 (World Health Organization, 2023; Walton et al., 2020). Its causes are not fully understood, but it is believed to result from a combination of genetic, viral, and environmental factors (Wingerchuk, 2012). This disease is more common in women than in men and has a lower incidence in regions closer to the equator (Walton et al., 2020).

In clinical terms, MS can be classified into different subtypes, based on the disability and activity level (World Health Organization, 2023).

Diagnosis of Multiple Sclerosis is a complicated task since it cannot be performed based on a single test. It involves a range of tests, including symptomology, blood analysis and image analysis (World Health Organization, 2023).

Medical Resonance Imaging (MRI) is crucial for diagnosing and evaluating diseases, as it is the only imaging technique that is able to enhance inflammatory states in soft tissues such as the brain and spinal cord (World Health Organization, 2023).

1.2. Role of MRI in MS Diagnosis

Magnetic Resonance Imaging (MRI) is a non-invasive medical imaging technique used to visualize detailed internal structures of the body. Unlike X-rays or CT scans, MRI does not use ionizing radiation. Instead, it employs a powerful magnetic field, radio waves,

and a computer to produce high-resolution images of organs, tissues, and skeletal structures.

The protons in water molecules within the body are aligned using a strong magnetic field to create these detailed internal images. When subjected to radio waves, these aligned protons produce signals that the MRI machine detects. A computer then processes these signals to create detailed images of the inside of the body. This technique is especially useful for imaging soft tissues and the nervous system, making it invaluable for diagnosing a variety of conditions.

MRI is crucial in diagnosing and monitoring of Multiple Sclerosis (MS), an autoimmune disease that affects the brain and spinal cord. MS causes lesions or scars in the central nervous system, which MRI can detect even before symptoms appear. MRI's ability to track changes in the brain and spinal cord over time also aids in monitoring disease progression and evaluating treatment efficacy.

In the context of MRI, T1 and T2 refer to two different types of images generated based on the relaxation times of the protons in the body's tissues after they have been excited by radiofrequency waves: T1-weighted images: These images are useful for visualizing the anatomy of the brain and the distinction between grey and white matter. In T1 images, areas affected with MS lesions may appear darker than the surrounding healthy tissue, aiding in the identification of damaged areas. T2-weighted images are particularly sensitive to fluid in tissues and are therefore excellent at highlighting areas of inflammation, edema, and lesions. In the context of MS, T2-weighted images can reveal lesions as brighter spots, providing valuable information about the extent and distribution of disease activity within the brain and spinal cord.

Together, T1 and T2-weighted MRI images provide comprehensive information that is crucial for diagnosing MS, understanding its progression, and guiding treatment decisions.

1.3. Challenges in Lesion Segmentation

In the field of medical imaging, specifically in relation to conditions such as Multiple Sclerosis (MS), lesion segmentation is crucial for diagnosis and treatment planning. This process involved identifying and outlining pathological lesions from healthy tissue in

imaging studies, such as MRI. Despite the benefits of technological advancements, this process remains complex and requires careful consideration when integrating into clinical practice.

Lesion segmentation poses a significant challenge due to the inherent variability in lesion appearance, including differences in size, shape, and signal intensity. Sophisticated algorithms are required to accurately classify a wide range of lesion presentations and ensure reliable segmentation across various clinical scenarios. Automated segmentation methods often struggle to differentiate between genuine pathological changes and imaging artifacts or normal anatomical variations, resulting in a higher rate of false positives. This can lead to an overestimation of the disease burden, which may negatively impact clinical decision-making and patient management strategies.

The task of segmentation task is made more challenging by the intricate anatomy of the brain, which presents significant obstacles due to the subtle differences between certain pathological lesions and normal structures pose significant hurdles. Therefore, the algorithms used for this purpose must have advanced interpretive capabilities to navigate this complexity effectively. Furthermore, the interpretation of medical images is subjective, which can lead to variations in assessments of images, among expert radiologists. This variability among observers makes it difficult to establish a consistent ground truth for training and validating machine learning models.

Additionally, the lack of standardized imaging protocols across different institutions adds another layer of complexity. Inconsistencies can affect the appearance of lesions on MRI scans, which can make it challenging to develop reliable and generalized segmentation algorithms across diverse datasets. Additionally, the availability of extensive, annotated datasets is crucial for the development of accurate segmentation models. However, collecting such data is limited by privacy concerns and the labor-intensive nature of manual annotation, which constrains the pool of high-quality data necessary for model training and validation.

Clinical requirements often necessitate the rapid processing and analysis of imaging data. However, the computational intensity required by advanced segmentation algorithms may hinder their practical application in real-time clinical settings. Therefore, computational efficiency improvements are necessary. Furthermore, it is a significant challenge to ensure that segmentation models can be adapted to different patient populations and datasets

obtained under varying imaging protocols. Therefore, it is crucial to design models are flexible and adaptable. Models that perform well in one setting may not necessarily maintain the same level of accuracy when introduced to new conditions.

Overcoming these multifaceted challenges requires a collaborative effort that spans ongoing research and interdisciplinary collaboration. Promising pathways to success include advances in computational methods, particularly within the realm of deep learning, alongside improvements in data accessibility and computational infrastructure. However, it is important to approach this task with cautious regarding ethical considerations and privacy concerns related to the use of medical imaging data. The ultimate goal is to ensure that advancements in lesion segmentation leads to tangible benefits for patient care and treatment outcomes.

1.4. Advancements and Research Gaps

Advancements in medical image segmentation using convolutional neural networks (CNNs) represents a significant milestone in the biomedical field. CNNs enables the precise identification and delineation of various anatomical structures and pathologies in imaging studies, facilitating improved diagnosis, treatment planning, and monitoring of diseases. CNNs have demonstrated their proficiency in handling the complexity and variability present in medical images, such as those obtained from computed tomography (CT) scans and magnetic resonance imaging (MRI).

A significant development in this field is the emergence of convolutional networks U-Net architectures. These models have set new benchmarks for accuracy in medical image segmentation tasks. They are capable of learning from a limited number of labeled images and generalizing well to new, unseen images, which is crucial in a field where annotated data are scarce and expensive to obtain. Moreover, techniques such as transfer learning and data augmentation have further enhanced the performance of CNNs in medical image analysis by leveraging pre-trained models and artificially enlarging the dataset, respectively.

Despite recent advancements, the field of medical image segmentation still faces significant research gaps. One of the primary challenges is the scarcity of publicly available, annotated medical imaging datasets. Obtaining such datasets is difficult due to

ethical considerations, patient privacy concerns, and the labor-intensive nature of medical image annotation. The limited availability of data impedes the creation and verification of new models, as machine learning algorithms, especifically deep learning models, require large amounts of data to achieve optimal performance.

Moreover, the heterogeneity of medical imaging data, resulting from differences in imaging modalities, protocols, and patient populations, presents a significant challenge. Developing models that are robust and generalizable across these variations remains a daunting task. This heterogeneity also makes it difficult to transfer models between institutions and imaging equipment, requiring extensive model retraining, and fine-tuning when applied to new datasets.

The interpretability of CNNs in medical image segmentation is an ongoing area of research. It is crucial to provide clinicians with understandable and trustworthy models for their adoption in clinical practice. Therefore, efforts to increase the transparency of CNN decision-making processes and to develop models that can provide explanations for their predictions are essential to bridge the gap between AI researchers and clinical practitioners.

1.5. Objectives and Contributions of the Thesis

This aim of this project is to develop an automated method for Multiple Sclerosis lesion segmentation on brain magnetic resonance imaging 2D T2-FLAIR modality. As this modality is commonly analyzed by physicians for diagnosing and assessing the evolution of Multiple Sclerosis lesions, it is crucial to develop tools to automate or semi-automate the process. Currently, there is no documentation on lesion detection or segmentation using this modality. The research aims to enhance the reliability of lesion detection and segmentation, which could lead to better monitoring of disease progression and treatment efficacy.

2. Literature Review

2.1. Multiple Sclerosis

Multiple Sclerosis (MS) is the most common neurological disability, according to the National Institute of Neurological Disorders and Stroke, a governmental organization in the United States of America -, Multiple Sclerosis. It is a chronic inflammatory disorder that damages the central nervous system (CNS), including the brain, spinal cord and optic nerves. MS is an autoimmune-mediated disease that can result in several physical or cognitive disability and neurological defects (National Institute of Neurological Disorders and Stroke, n.d.). Notably, it is characterized by the presence of lesions or plaques in the CNS, which result from a process named demyelination - a process in which the protective covering of nerve fibers is damaged (Ghasemi, et al., 2017).

Although the etiology of MS is not completely understood, it is believed to involve a combination of genetic susceptibility and environmental factors, such as smoking (Wingerchuk, 2012) and/or the contraction of different types of viral infections, such as the infection by the Epstein-Barr virus (Compston & Coles, 2008). In addition, females are two to three times more likely to be diagnosed with MS compared to the male counterpart. This phenomenon suggests a hormonal contribution to the development of the neurologic disease. (Walton, C., et al., 2020)

2.1.1. Symptoms and Progression

The symptoms of MS can vary greatly, ranging from numbness and tingling to more severe impairments such as impaired speech and swallowing. Table 2.1 provides a summary of the diverse manifestations of MS. Common symptoms include movement and coordination difficulties, hearing impairment, fatigue, and impaired vision. Furthermore, some individuals may suffer from bladder difficulties, sexual dysfunction, cognitive issues, and pain (Multiple Sclerosis International Federation, 2013).

Table 2. 1 - *M*S Symptoms (Seminar 1502 www.thelancet.com Vol 372 October 25, 2008 Multiple sclerosis Alastair Compston, Alasdair Coles)

Localization	Symptons	Signs
Cerebrum	Cognitive impairment	Deficits in attention, reasoning, and executive function (early), dementia (late).
	Hemisensory and motor Affective (mainly depression) Epilepsy (rare) Focal cortical deficits (rare	Upper motor neuron signs
Optic Nerve	Unilateral painful loss of vision	Stocoma, reduced visual acuity, color vision, and relative afferent pupillary defect
Cerebellum and cerebellar pathways	Tremor	Postural and actional tremor, dysarthria
	Clumsiness and poor balance	Limb incoordination and gait ataxia
Brainstem	Diplopia, oscillopsia	Nystagmus, internuclear and other complex ophthalmoplegias
	Vertigo Impaired swallowing Impaired speech and emotional liability Paroxysmal symptoms	Dysarthria Pseudobulbar palsy
Spinal Cord	Weakness Stiffness and painful spams Bladder dysfunction Erectile impotence Constipation	Upper motor neuron signs Spasticity
Others	Pain Fatigue Temperature sensitivity and exercise intolerance	

Based on the evolution and symptoms manifestation, the disease progression may be categorized into the subsequent types, namely:

1) RRMS - Relapsing–Remitting Multiple Sclerosis
2) SPMS - Secondary Progressive Multiple Sclerosis
3) PPMS - Primary Progressive Multiple Sclerosis

Relapsing-remitting multiple sclerosis (RRMS) is the most prevalent type, accounting for 85% of the cases. Patients experience relapses followed by recovery. Eventually, 35 to 50% of RRMS patients progress to secondary progressive multiple sclerosis (SPMS), which is characterized by slow neurological deterioration (Meca-Lallana et al.,2021). The evolution of the disease from RRMS to SPMS is described in the following figure from the National Society of USA, 2023.

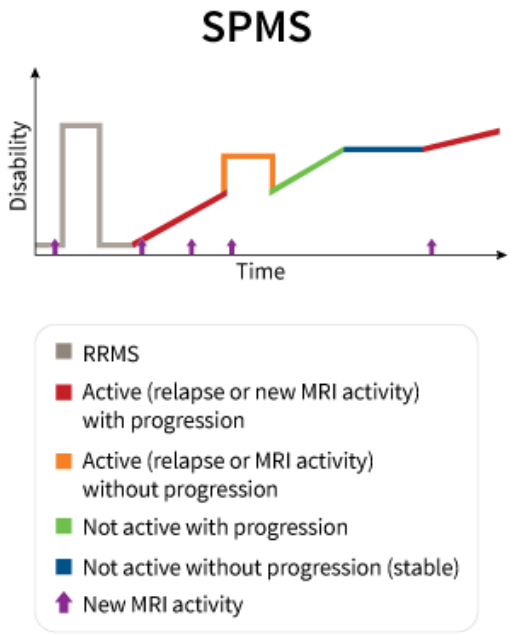

Figure 2. 1 **-** Graph depicting SPMS evolution over time.

Around 15% of multiple sclerosis (MS) patients show primary progressive MS (PPMS) from the onset, marked by gradual worsening without relapses (Meca-Lallana et al.,2021).

2.1.2. Central Nervous System and MS Pathogenesis

The central nervous system (CNS) is composed of the brain and spinal cord, while the peripheral nervous system includes all other nerves. The central nervous system is responsible for receiving, processing, and responding to sensory input, throughout a specific type of cells, named neurons, shown on Figure 2.2. Neurons communicate and propagate stimulus through synapses. Synapse is the process of transmission of electrochemical stimulations from synaptic end bulbs to the adjacent neuron dendrites. A group of neurons is called neural network (Thau, et al., 2022).

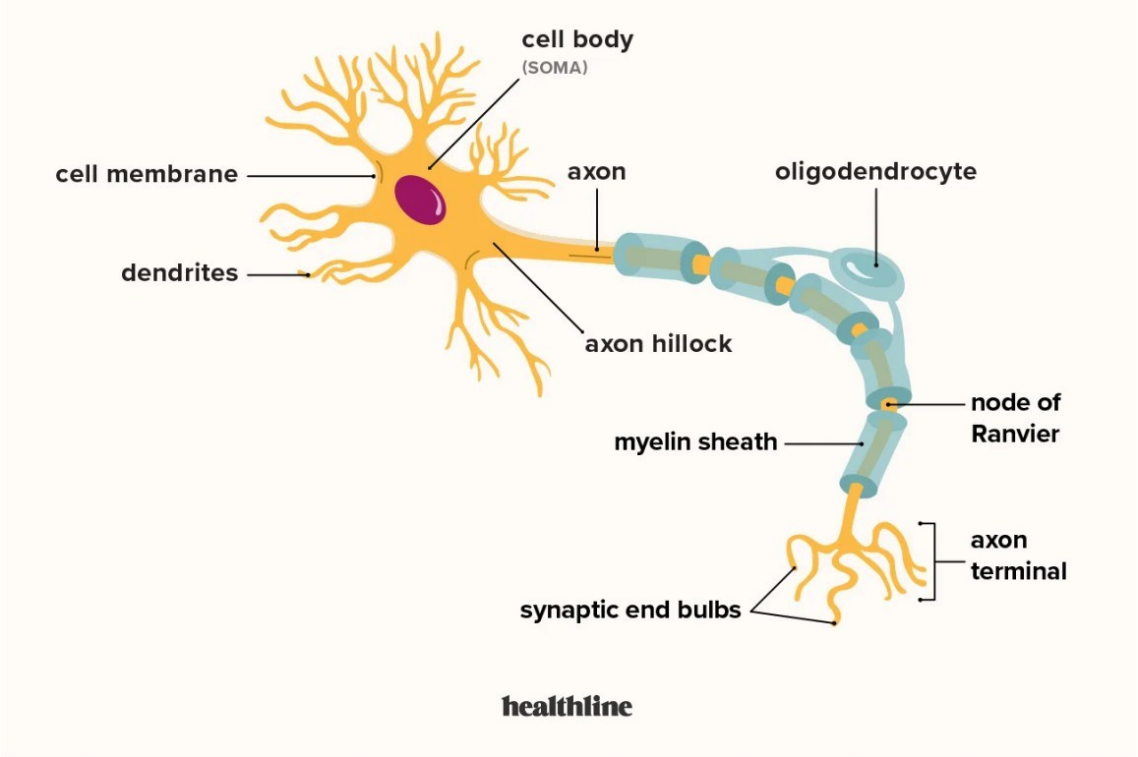

Figure 2. 2 - Representation of a neuron structure.

The nuclei of neurons are located in the cell body. Dendrites extend from the cell body to the adjacent axon, which has stronger and longer structures (see Figure 2.2, Vandergriendt, C., Zimlich, R., 2022). Electrical impulses are transmitted along the axon, activating the subsequent neuron upon arrival. Some axons are myelinated, meaning they are surrounded by a myelin sheath. This myelin sheath is, a multi-layered lipidic and protein structure, produced by oligodendrocytes, which isolates the axon and consequently increases signal propagation speed. The gaps between the myelin sheaths

enclosing axons are referred to as nodes of Ranvier. In this context, when an action potential is initiated, an ionic current flow passes rapidly through the myelin sheaths, causing depolarization. This phenomenon results in a signal jump between nodes, which consequently triggers the next node's action potential. It is important to note that, the low conductivity of myelin prevents the electrical signals from being lost to the surrounding tissue (Shah, Abbruscato, 2017).

Regarding myelin concentration, Figure 2.3 show the variation in colour of the different parts of the human brain. The white matter (WM) contains the higher concentration in myelin of the human brain. The WM whitish appearance results from presence of high myelin concentrations. Contrary, grey matter (GM), it involves the brain's surface and contains neural cell bodies, dendrites, and unmyelinated axons in its composition, lacking due to the absence of myelin in color. Additionally, the brain can be sectioned into three parts, namely cerebrum, cerebellum, and the ventricles, which are situated on the brain's center and contain the Cerebrospinal Fluid (CSF) (Shah, Abbruscato, 2017).

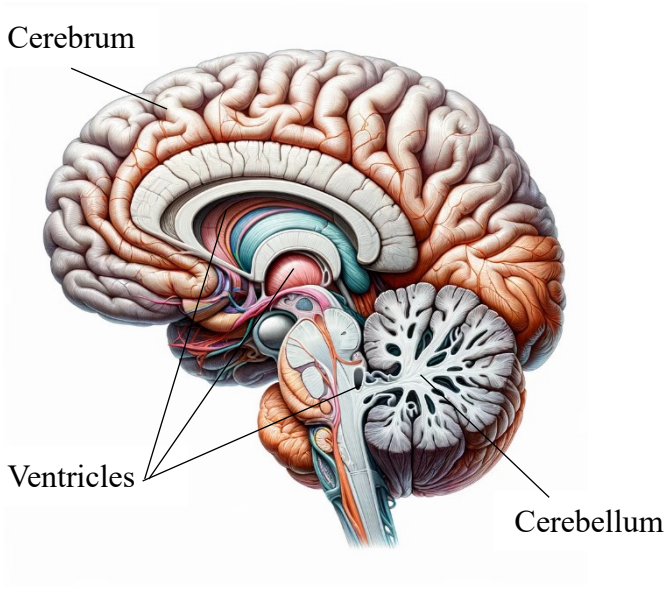

Figure 2. 3 – Brain's Anatomy Illustration

The capillary walls of the CNS form the blood-brain barrier (BBB), which regulates the exchange of ion and molecules between the blood and CNS. The BBB is highly regulated and selective when compared to other counterparts of the microvascular system, due to its unique endothelial cells. This barrier is crucial for proper neural function and nervous system protection (Hauw, et al., 1992; Shah, Abbruscato, 2017)

Multiple Sclerosis pathogenesis is characterized as an autoimmune condition which triggers an abnormal immune response against its own tissue. Hereby, this trigger causes demyelination along the axons, resulting, consequently, in the disruption of nerve impulses' propagation. This disruption may lead to the symptoms mentioned in section 2.1.1 (Avila, et al., 2017).

The loss of oligodendrocytes results in the degeneration of myelin, hindering the maintenance of the myelin layer. With the disease's progression, two phenomena may occur, namely damage of the myelin sheaths and of the axons, resulting in an impediment of electrical signals transmission. In the early stages of the disease, oligodendrocytes have the ability to remyelinate axons, however this restorative process does not endure, leading to disease progression into the SPMS stage (Costa, et al., 2023).

The disruption of the BBB during MS leads to increased permeability, allowing migration of lymphocytes into the CNS. The T and B cells which migrated to the CNS, undergo an autoimmune response, i.e., it attacks the CNS by targeting the myelin. Although not fully understood, this autoimmune response will trigger further reactions. Specifically, B-cells secrete immunoglobulins, which proliferate in the CNS, while T-cells initiate myelin degeneration. For instance, during MS diagnosis, an elevated number of B-cells in the oligoclonal bands can be found (Dobson, Giovannoni, 2019; Costa, et al., 2023).

2.1.3. Diagnosis

Diagnosing multiple sclerosis is a time-consuming and costly process that cannot be achieved through a single test. The diagnosis may be particularly arduous due to the lengthy wait times in the Serviço Nacional de Saúde and the targeted analyses required. As outlined in Chapter 2.1.1, the symptoms of MS can vary greatly and persist for an undetermined length of time. It is not uncommon for patients to initially overlook these symptoms, only seeking medical attention once an obvious sign, such as vision loss,

becomes apparent. From there, the physician will likely order a range of tests, including a lumbar puncture to screen for oligoclonal bands, blood tests for antinuclear antibodies (ANAs), and other diagnostic measures to rule out alternative conditions. Ultimately, magnetic resonance imaging plays a crucial role in confirming a MS diagnosis.

After compiling all the results, the physician begins a preliminary diagnosis and brings it to a council for further evaluation. Together, they validate the initial diagnosis and collaborate on potential treatments for the individual patient. The provided diagram illustrates the sequential process of diagnosing MS.

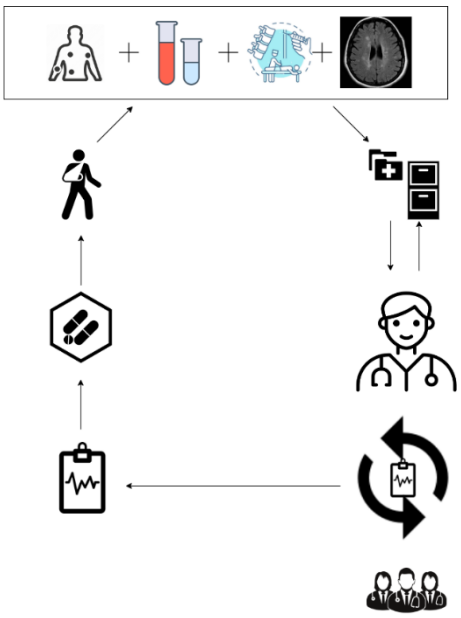

Figure 2. 4 **-** Multiple Sclerosis Diagnosis Protocol

The McDonald Criteria are an internationally approved diagnostic method for MRI that is followed in 96% of countries worldwide (Thompson AJ, 2018).

These criteria require the presence of inflammations in typical and different MS-associated sites over a certain period, known as dissemination in time and space. At least two different time instances are necessary to fulfill the criteria for dissemination in time. To achieve this, an MRI scan can be conducted to search for active lesions that are enhanced by an injection of gadolinium contrast (Thompson AJ, 2018)

In patients with MS, lesions are commonly found in the cortical, infratentorial, juxtacortical, periventricular, or spinal cord regions. If a patient has experienced only one attack, known as clinical isolated syndrome (CIS), a cerebrospinal fluid (CSF) examination should be conducted. Oligoclonal bands can be detected through protein electrophoresis and have been validated as a reliable indicator of a subsequent attack (Thompson AJ, 2018).

Table 2. 2 - Mc Donald Criteria, 2017. Adapted from Thompson AJ, Banwell BL, Barkhof F, et al. Diagnosis of multiple sclerosis: 2017 revisions of the McDonald criteria. Lancet Neurol. 2018;17:162-73.

Clinical Presentation	Additional Data Needed for Diagnosis
≥ 2 clinical attacks and objective evidence of ≥ 2 lesions	None
≥ 2 clinical attacks and objective evidence of 1 lesion	DIS: an additional attack implicating a different CNS site OR by MRI[a]
1 clinical attack and objective clinical evidence of ≥ 2 lesions	DIT: an additional clinical attack OR by MRI[b] **OR** CSF-specific oligoclonal bands
1 clinical attack and objective evidence of 1 lesion	DIS: an additional clinical attack implicating a different CNS site OR by MRI[a] **OR** DIT: an additional clinical attack OR by MRI[b] **OR** CSF-specific oligoclonal bands

[a]*DIS by MRI: new lesions on follow-up imaging or both gadolinium-enhancing and non-enhancing lesions on single MRI.*

[b]*DIS by MRI: > 1 symptomatic or asymptomatic lesion in > 2 areas including cortical/juxtacortical, periventricular, infratentorial, or spinal.*

2.1.4. MS Treatment

Currently, there is no cure for MS. However, disease-modifying therapies (DMTs) are widely used to alleviate MS symptoms. There are various types of DMTs, all of which share the common trait of modulating or suppressing the immune system. These agents can be administered orally or through alternative routes, such as injection or infusion. The aim of these treatments is to reduce the number of relapses and delay the progression of the disability. Medications for MS can be classified based on their effectiveness, as either

moderate or high, or as 1st line and 2nd line treatments (Kuhlmann, Antel, 2023). Corticosteroids are also frequently used to reduce inflammation during MS flare-ups (Kuhlmann, Antel, 2023).

The table below describes the currently available medications for managing MS, according to Dasgupta et al. (2019).

Table 2. 3 – Multiple Sclerosis current treatment pharmaceuticals

Medications	**Administration**	**Purpose**
Methylprednisolone	Intravenous	Reduce inflammation
Prednisolone	Oral	Managing the relapse
ACTH	Injection	Acute exacerbation
Interferon beta	Injection	Modify the course
Glatiramer acetate	Injection	Modify the course
Teriflunomide	Oral	Delay the progression
Fingolimod	Oral	Delay the progression
Dimethyl fumarate	Oral	Delay the progression
Alemtuzumab	IV infusion	Inhibit immune cell to cross BBB
Natalizumab	Infusion	Inhibit immune cell to cross BBB
Mitoxantrone	Infusion	Inhibit immune cell to cross BBB
Ocrelizumab	Intravenous infusion	Block CD20 + ve lymphocytes
Hematopoietic stem cells	Transplantation surgery (chronic progressive stage)	*De novo* generation of naive lymphocytes to reduce autoimmunity

DMTs are no effective in treating or improving symptoms in PPMS patients. However, studies and clinical trials have shown that these treatments have a significant and beneficial impact on RRMS and SPMS cases. MS treatment is complex due to the disease's atypical nature and the various side effects that are specific to each patient. Individual with MS may require additional medication to address specific symptoms such as muscle stiffness, pain, and bladder issues (Kuhlmann, Antel, 2023).

To avoid axonal damage, treatment must begin promptly in cases in which the patient is diagnosed with PPMS. For these specific cases, symptomatic treatment and physical

therapy are administered instead. At present, the only drug that has been proved to be able to stop disease progression is Ocrelizumab (Lamb YN, 2022).

2.2. Magnetic Resonance Imaging

Magnetic Resonance Imaging (MRI) is a non-invasive diagnostic tool that has revolutionized medical imaging. By leveraging the principles of nuclear magnetic resonance, MRI provides detailed images of the body's internal structures, particularly soft tissues, including the brain, muscles, and heart.

The core principle of MRI is based on the alignment of hydrogen atoms in the body when placed in a strong magnetic field. When exposed to a radiofrequency (RF) pulse, these hydrogen atoms absorb energy and transition to a higher energy state. Upon cessation of the RF pulse, the hydrogen atoms return to their original state, releasing energy in the process. RF coils detect this energy and translate it into images (Kwok, 2022; Azhar & Chong, 2022).

RF coils are essential components of MRI systems as they transmit the RF pulse to the patient's body and receive the signals emitted by hydrogen atoms. The design and selection of RF coils are crucial for achieving high-quality images. The choice of coil depends on the body part being imaged and the specific requirements of the imaging technique (Kwok, 2022).

Hydrogen protons are highly prevalent in both water and fat. This characteristic is useful for detecting inflammation because water tends to accumulate in regions prone to inflammation. Therefore, MRI can be rendered as a sensitive diagnostic technique (Brown et al., 1999).

All elementary particles possess an innate attribute called spin, which denotates their rotation around an axis. As a moving charge, the spin indicates the presence of a magnetic field surrounding the particle. Therefore, the proton rotates around the axis of the magnetic field (Brown et al., 1999).

The patient is positioned inside the magnetic resonance (MR) scanner, where a strong magnetic field (B_0) is active. The protons align with B_0, due to the magnetic field, resulting in the creation of a net magnetization (M_0). Equation 2.1, which represents the Larmor

equation, shows that the precession frequency of the protons adjusts to B0, where γ represents the gyromagnetic ratio of the hydrogen atom (Brown et al., 1999).

$$\omega_0 = \gamma B_0, \text{ where } \gamma = 42,57\text{MHz/T}$$

Equation 2. 1 - Larmor Equation

Measurement in the direction of the body's net magnetization is impossible due to its substantially smaller size compared to the external magnetic field. Therefore, the signal is evaluated in the transverse plane using a radio frequency (RF) pulse. The RF pulse vibrates at the designated Larmor frequency and is generated by the transmit coil, which functions as a stable magnetic field B_1, on the impacted protons. B_1 is perpendicular to B_0, causing the protons and therefore M_0 to rotate into the transverse plane (Brown et al., 1999).

The flip angle, α, can be calculated using Equation 2.2:

$$\alpha = \gamma B_1 t_p$$

Equation 2. 2 - Angle α Calculus

A flip angle of 90º is often achieved by adjusting the pulse duration, *tp*. This will result in a coherent spin pattern caused by the RF pulse. M_0 induces a current in the transmit coil, where the signal's voltage is measured. The signal exponentially decays, and M_0 slowly aligns with B_0 upon switching off the RF pulse. During relaxation to the initial state, the relaxation times T_1 and T_2 are measured. T_1 is the length of time necessary to reach 63% of the initial magnetization and it varies across the various tissue types. Similarly, T_2 is defined as the time required for the protons to diphase in the transverse plane (Brown et al., 1999).

Conventional contrast-weighted images are created through various pulse sequence compositions, which entail the emission of RF-pulse and gradient pulses, generated with specific patterns and timing (Brown et al., 1999).

Pulses are emitted with a predetermined pattern and timing. The parameters repetition time (TR) and echo time (TE) dictate when measurements are taken. Thus, adjusting these allow desired tissue contrast achievement (Brown et al., 1999).

To determine the spatial position of the signal, gradients may be added to the magnetic field. According to Equation 2.1, it is known that a modification in the static field B_0 results in a frequency alteration. The variation in the gradient field in each position is recognized. The receiver is tuned into only detecting a specific frequency and it is, therefore, possible to determine where the signal has derived (Brown et al., 1999).

Several advanced techniques have been developed to enhance the capabilities of MRI. Zero echo-time (ZTE) MRI, for instance, is designed to capture signals from short-T2 tissues and is particularly useful in imaging cortical bone and complex brain structures. Another significant advancement is Electrical Properties Tomography (EPT), which images the electrical properties of tissues, providing insights into their physiological and pathological states (Wiesinger & Ho, 2022; Liu et al., 2017).

These new techniques may work very well, however in order to ensure accurate diagnosis it is crucial to address artifacts that may arise from patient motion, magnetic field inhomogeneities, and issues with RF, which may affect signal-to-noise ratio, uniformity, and resolution of the images (Kwok, 2022).

The use of MRI spans a wide range of clinical applications, including imaging of the brain, spinal cord, musculoskeletal system, heart, and abdomen. Concerning brain imaging, MRI plays a critical role in identifying conditions such as tumors, stroke, and neurodegenerative diseases. It also has great value in the study of brain function and structure in research settings (Azhar & Chong, 2022; Miller et al., 2016).

Although MRI is generally considered safe, it does have its limitations. For example, individuals with implanted metallic devices, such as pacemakers, may not be eligible for this type of scan. Furthermore, the use of contrast agents, which are necessary for certain MRI exams, could potentially pose risks for patients with certain health conditions (Kwok, 2022).

Resuming, MRI is a sophisticated imaging modality that combines advanced physics, engineering, and computer science to provide detailed images of the body's internal structures. Ongoing advancements in MRI technology continue to expand its diagnostic capabilities and applications.

2.3.MS Findings on MRI scans

To fully understand the characteristic MRI findings in MS, it is important to consider several key-poins. These include the association with pathological imbalance, location, sleep-related disorders, and cognitive function of the patient.

Brain and spinal cord lesions caused by MS show a strong correlation with pathological changes, indicating the areas where the myelin sheath has been damaged. T2Weighted (T2W) FLAIR is a commonly used method for detecting MS lesions due to their significant contrast appearance. Inflammation causes water accumulation, resulting in a hyperintense appearance due to a decreased R2 rate (Filippi et al., 2019; Filippi et al., 2012). However, one disadvantage of the T2W contrast weighted image is its inability to characterize disease activity. The hyperintense appearance may indicate inflammation, oedema, or axonal loss, however the distinguishment between these conditions is not possible (Sahraian et al., 2010, Barkhof & van Walderveen, 1999). As a result, there is a weak correlation between disability and T2W lesion load. Nevertheless, T2W contrast is valuable for meeting the criteria of dissemination in space during the diagnosis process.

Disease activity is assessed using gadolinium, a paramagnetic substance that acts as a contrast agent. Gadolinium accumulation in active lesions in the T1W image results in a hyperintense appearance due to the shortened T1 relaxation (Filippi et al., 2019; Filippi et al., 2012, Barkhof & van Walderveen, 1999). This shortened relaxation time indicates a disruption of the BBB, and consequently, a lesion in an early inflammatory stage (Barkhof & van Walderveen, 1999). Unenhanced T1-weighted (T1W) lesions may appear hypointense or isointense but are consistently hyperintense in T2-weighted imaging (Sahraian et al., 2010). All lesions experience this stage of activity, which lasts for 2-8 weeks before the BBB damage is repaired. The active lesions indicate destruction of myelin [20], with long-standing active lesions posing a higher risk of progression to persistent *black holes*. Unenhanced T1-weighted lesions are hypointense and commonly referred to as black holes (Sahraian et al., 2010). The decreased signal arises from an increase in the extracellular space caused by axonal loss and oedema. Several T1-weighted lesions are isointense; hence, not visible on the image. Most of lesions exhibit evidence of irreversible tissue damage and are associated with a greater degree of clinical disability than the T2-weighted lesion load (Sahraian et al., 2010, Barkhof & van Walderveen, 1999). While some black holes may persist, others may disappear over time, indicating the possibility of repair and remyelination. Black holes are more prevalent in

progressive multiple sclerosis stages than in relapsing-remitting MS (RRMS), which is likely due to greater neurodegenerative activity (Barkhof & van Walderveen, 1999).

In the brain, MS lesions are typically found in the periventricular, juxtacortical and infratentorial regions. One well-known finding in MS patients' MRI scans is the presence of Dawson's fingers (as shown in Figure 2.5, Abdelmonem H, n.d), which are periventricular lesions that extend into the brain parenchyma and are a distinctive feature of MS. Spinal cord lesions are also common, often affecting the cervical and thoracic regions (Lopaisankrit & Thammaroj, 2023).

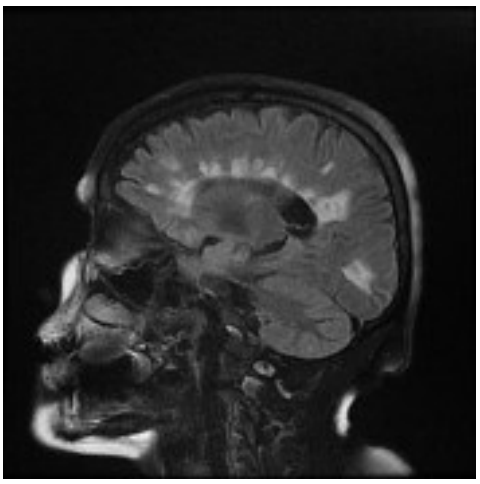

Figure 2. 5 - Appearance of the MS characteristic feature Dawnson's Fingers on a 30y old Female MRI diagnosed with Multiple Sclerosis

New evidence of a relationship between sleep-related disorders and MRI findings is emerging in the context of MS. This association highlights the multifaceted nature of MS and the importance of a comprehensive approach to patient management (Foschi et al., 2019).

Furthermore, advanced MRI techniques have been used to study the correlation between MRI findings and cognitive functions in MS patients. Asadollahzadeh et al. (2023) found significant correlations between certain neuropsychological tests and MRI metrics, highlighting the impact of MS on cognitive abilities.

Moreover, studies have demonstrated variations in MRI characteristics of MS among different populations. For example, Thai MS patients exhibit some differences in MRI

findings compared to Western populations, suggesting potential variations in disease manifestation (Lopaisankrit & Thammaroj, 2023).

In conclusion, MRI is an invaluable tool in the diagnosis and management of MS, providing insights into the extent and progression of the disease. Understanding the MRI characteristics of MS is crucial for clinicians in devising appropriate treatment strategies and managing patient outcomes.

2.4. Machine Learning and Artificial Neural Networks

Artificial Neural Networks (ANNs) are computational models inspired by the human brain. They mimic the synapses and networks created by biologic neurons (section 2.1.2) and comprise groups of interconnected artificial neurons for computation and data processing. The main concept behind ANNs is the simulation of the brain's ability to recognize and handle patterns (McCulloch & Pitts, 1943).

The fundamental component of an ANN, akin to CNS, is the neuron. In this context, the neuron is a mathematical function, represented as:

$$z(x) = \left(\sum_{i=1}^{n} (x_i w_i) + b \right)$$

Equation 2. 3 **-** Neurons' Equation

The output of the neuron is represented by z in the equation. w refers to the weight, x is the input, and b is the intercept term, also known as bias.

An artificial neural unit calculates the weighted sum of inputs, where w represents the synaptic strength and x represents the inputs from other neurons or sensors. The activation function, denoted by $f(x)$, is a non-linear function that acts as the threshold function within biological neurons. Furthermore, the activation function will output a real number based on the nucleus potential (Habibi Aghdam and Elnaz Jahani Heravi, 2017).

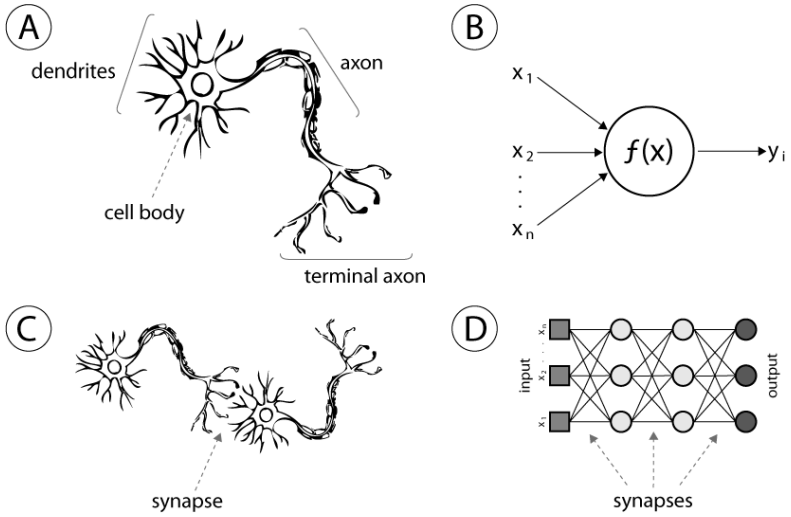

Figure 2. 6 - (A) Human neuron; (B) artificial neuron or hidden unity; (C) biological synapse; (D) ANN synapses (Handican, 2019)

Figure 2.6 (B) shows a simplified version of the biological element depicted in Figure 2.6 (A). This analogy comprises neuron, a fundamental building block present in every artificial neural network. The differences in signal weighting at synapses, the interconnections, are visible (see Figure 2.6 (D)). The neural structure consists of dendrites, which receive multiple inputs with distinctive weights, a cell body that calculates the weighted sum of inputs, and an activation function represented by the axon. The axon defines the threshold responsible for propagating the signal, and the output is represented by the axon terminals (Suzuki, 2013). The axon defines the threshold responsible for propagating the signal, and the output is represented by the axon terminals (Suzuki, 2013). The axon defines the threshold responsible for propagating the signal, and the output is represented by the axon terminals (Suzuki, 2013).

Like everything in the scientific world, the development of an artificial neural network has its advantages. These include the ability to choose the most suitable architecture for the intended purpose, as well as the activation and loss functions.

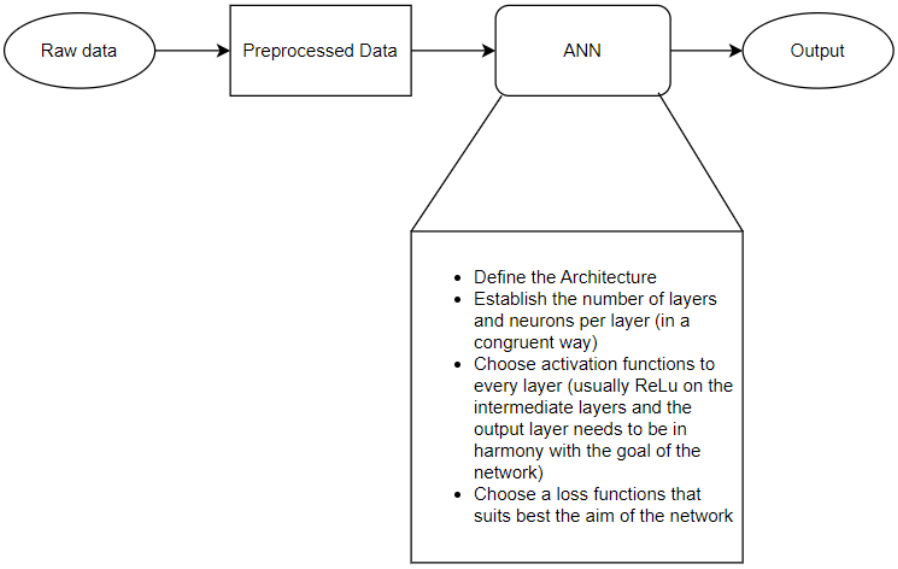

Figure 2. 7 **-** Simplified description for an ANN development.

The perceptron is the simplest neural network, consisting of a single input layer and an output node (see Figure 2.8). It calculates a weighted sum of neuron inputs and produces an output of 1 if this sum exceeds the activation threshold. Therefore, a single perceptron is useful when fitting a straight line into a scatter plot (X, Y), where X represents the input and Y represents the output variables, respectively. Furthermore, if the data is represented by two populations that can be divided by a straight line, then a single perceptron would be sufficient to separate them. For example, it could be used as a linear classifier (as shown in the Figure above).

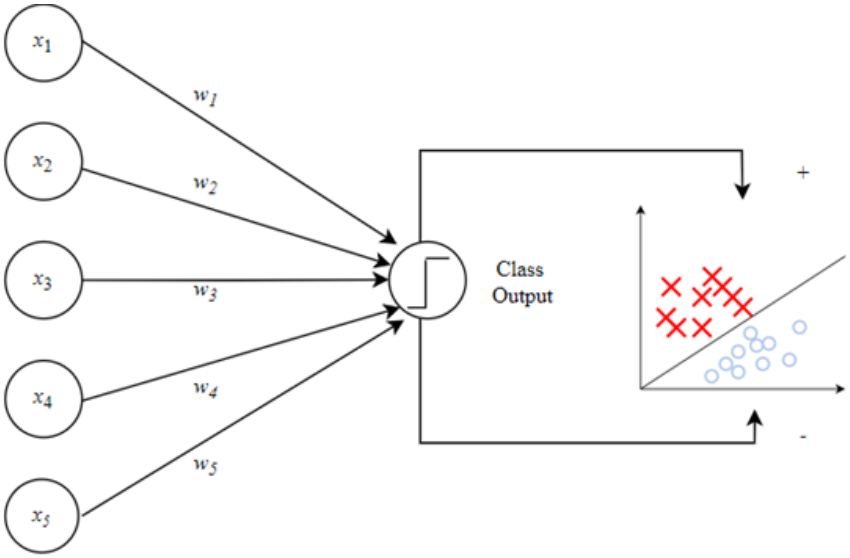

Figure 2. 8 - Perceptor Algorithm (Durstewitz, et al., 2019)

Suzuki (2013) stated that a perceptron, which is a one-layer feed-forward neural network, is limited to solving linear problems. The number of perceptrons required to fit our data can be derived from the number of hyperplanes needed to separate the existing subsets of the population. This requirement increases with the dimensionality of the data. The number of perceptron's will increase, leading to a single-layer network with perceptron's as the nodes, when dealing with nonlinear behavior or even be extend to a fully-fledged multilayer neural network.

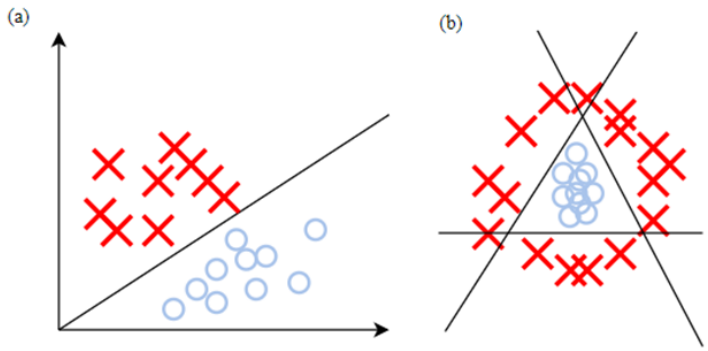

Figure 2. 9 - (a) Linear Perceptor for binary classification; (b) Non-linear Perceptor for binary classification.

A Figure 2.9 (b) illustrates a biological network, which is a multilayer neural network. Similarly, an artificial neural network comprises of multiple computation layers, including intermediate layers (between input and output), also known as hidden layers. These computations are not visible to users (Aggarwal, 2018).

Neurons in a neural network can be connected or disconnected, and the type of connection determines the network's behavior. There are two main categories are feed-forward "vanilla" and recurrent neural networks (as shown in Figure 2.10 below). In a feed-forward neural network, the connections between neurons do not form a cycle. In contrast, recurrent neural networks have connections between neurons that create a directed cycle (Pekel and Kara, 2017). The architecture of feedforward networks assumes that all nodes in one layer are connected to those of the next layer. Therefore, the neural network's architecture is almost entirely described once the number of layers and the number/type of nodes in each layer have been defined (Aggarwal, 2018). As convolutional neural networks are a specific type of feedforward network, this will be the focus point.

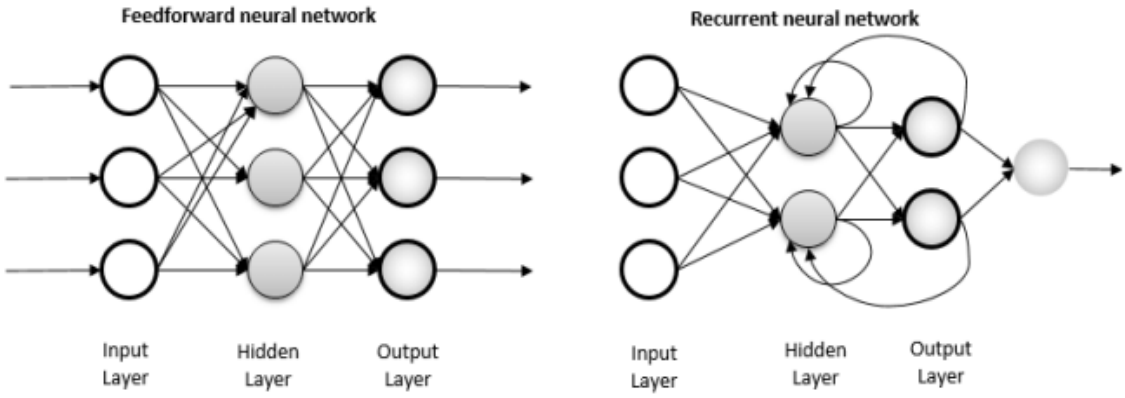

Figure 2. 10 - Feedforward and recurrent ANN architecture (Pekel and Kara, 2017)

The architecture of feed-forward neural networks comprises an (i) input layer, (ii) hidden layers, and an (iii) output layer. The input layer allocates the input data, with the number of neurons equal to the number of features. For instance, a signal with 224 pixels requires an input layer with 224 neurons. The output layer is responsible for classification or prediction values (Aggarwal, 2018).

In classification and segmentation problems, it is important to ensure that the number of neurons in the output layer should matches the number of classes. For instance, a network

designed to classify cars, planes, and boats must have three neurons in the output layer. In this work, for example, two output layers will be implemented: mask segmentation and no mask.

Selecting the number of neurons for the input and output layers is the initial stage in creating a feed-forward neural network. Other important parameters include the activation function, loss function; optimization method; number of hidden layers, layer connectivity, and number of units per layer (Goodfellow et al., 2016).

2.4.1. Activation Function

The selection of an appropriate activation function is a crucial aspect of neural network design. Activation functions introduce non-linearity to the output of the neuron, which is particularly important when scaling up from a single perceptron to a multi-layer architecture. There are several types of activation functions, including Linear, Sigmoid, Tanh, Hard Tanh, and ReLU, each used in different scenarios. Table 2.4 below displays representations of all the activation functions.

Table 2. 4 **-** Activation Functions (Sebastian Raskca, 2016)

Activation Function	**Equation**	**Example**	**1D Graph**
Linear	$\phi(z) = z$	Adaline, linear regression	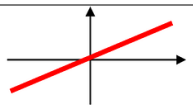
Logistic (Sigmoid)	$\phi(z) = \frac{1}{1 + e^{-z}}$	Logistic regression, Multi-layer NN	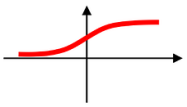
Hyperbolic tangent (Tanh)	$\phi(z) = \frac{e^{z} - e^{z}}{e^{z} + e^{z}}$	Multi-layer Neural Networks	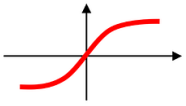
Rectifier, ReLU (Rectified Linear Unit)	$\phi(Z) = max(0, z)$	Multi-layer Neural Networks	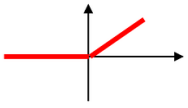
SofMax	$\phi = \frac{e^{z_i}}{\Sigma_k e^{z_k}}$	Multi-layer Neural Networks most used on output layer	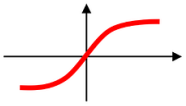

Where:

e^{z} is the exponential of the score for class
z_k represents each score in the vector z

The linear function is frequently used in the output layer of regression problems, where the target variable to be predicted is a real number.

The **Sigmoid/Logistic** activation function produces outputs between 0 and 1. The sigmoid output approaches 1 as the sum of the weights increases, and vice versa. This ensures that the output is always within the range of 0 to 1. Sigmoid activation layers are commonly used in multi-label classification problems (Graupe, 2013) as they ensure that the output is always within the range of 0 to 1, which can be interpreted as probabilities.

The **Tanh** function is similar to the sigmoid function, but it is vertically scaled to (-1, 1). The primary advantage of the hyperbolic tangent (Tanh) function over the sigmoid function is that it is zero-centered. This allows for the mapping of extremely negative, neutral, and highly positive values. values. Furthermore, the larger gradient (due to stretching) of the Tanh makes it easier to train (Suzuki, 2013).

Sigmoid and Tanh activation functions are primarily used at the output layer due to their computational expense. To reduce computational stress, **ReLU** and hard tanh were developed.

The Rectified Linear Unit (ReLU) is the most commonly used activation function in neural network architectures due to its widespread use. It converts all negative values to zero while maintaining positive values. ReLU is a unique activation function that only activates neurons with positive inputs, making it more computationally efficient than other activation functions. Other activation functions include Leaked ReLU, Parametric ReLU, GeLU (Gaussian Error Linear Unit), ELU (Exponential Linear Unit), and SoftMax (Aggarwal, 2018).

SoftMax is a function that converts the output layer's raw scores of the output layer into probabilities by exponentiating and normalizing each score. It is the most commonly used activation function for the output layer.

The selection of an appropriate activation function is critical for the neural network's performance. Nonetheless, optimization is a highly complex process due to the large number of functions and hyperparameters required.

2.4.2. Loss Function

Briefly, the loss function is an algorithm that evaluates the performance of the neural network. It assigns a high value if the predictions are completely wrong and a low value if they are accurate. This metric is used during backpropagation - It works by propagating the error backward through the network layers, adjusting weights to improve prediction accuracy to improve the model. The choice of the loss function is crucial for the learning process and depends on the classification or regression problem at hand. For regression problems, the simplest function is the squared loss, which is represented by $(y - \hat{y})^2$, where y is the "true value" and $\hat{y}$ is the prediction (Rumelhart et al., 1986). The Mean Squared Error (MSE) is the most commonly used measure of loss.

Mean squared error (MSE) is a regression loss function used to evaluate model performance when the target data is distributed around the mean value. It is sensitive to outliers and penalizes large errors more heavily than small ones due to its quadratic formula. Therefore, it is best suited for penalizing outliers (Graupe, 2013).

Mean Absolute Error (MAE) is another regression loss function that is similar to MSE, but instead of being quadratic, it is absolute.

The MAE function is not sensitive to outliers, making it suitable for scenarios where outliers do not significantly affect the results (Graupe, 2013). It can be applied to multimodal distributed data, where it is preferable to have predictions at one of the nodes rather than at the mean of them. Steep gradient slope can pose significant drawbacks, as minor errors can lead to convergence problems, or the large gradient might result in divergence. Conversely, a small slope may lead to slow convergence or cause the gradient to vanish. Concerning multi-label classification, a well-known loss function is Categorical Crossentropy.

In classification problems, the length of the output layer corresponds to the number of classes. The predicted probability of belonging to each category is contained in $\hat{y}_i$. To compare the predicted probability with the true probability, categorical cross-entropy is used. The negative sign in the equation ensures that the loss decreases as the predicted probabilities approach the target probabilities (Aghdam and Heravi, 2017). Therefore, as the output layer represents probabilities, the categorical cross-entropy is used to compare the predicted and true probabilities.

Moreover, Binary Crossentropy is a loss function used for binary classification problems, where there are only two possibilities such as Yes/No or 0/1. The formula is similar to categorical crossentropy, as the principle remains the same.

The loss function should calculate log $(1 - \hat{y}_i)$, which requires $\hat{y}_i$ to be between 0 and 1. Therefore, the output layer's activation function must be the sigmoid, as it is the only function that ensures independent outputs within this range (Aggarwal, 2018).

Binary Crossentropy may be useful in segmentation problems, by probabilistically assigning pixel values to 0 or 1. However, **Dice Loss** is more commonly used in segmentation tasks. Dice Coefficient ranges from 0 to1, with 1 indicating complete similarity and 0 indicating poor similarity (Jadon, S., 2020). A summary of the loss functions can be found in Table 2.5.

Table 2. 5 **-** Loss Function Resume

Objective	Equation	Loss Function	Usage	Observations
Prediction	$\frac{1}{N}\sum_{i=0}^{N}(y_i - \hat{y}_i)\text{^}2$	MSE	Data with normal distribution around the mean	
			Penalize outliers	
	$\frac{1}{N}\sum_{i=0}^{N}\lvert y_i - \hat{y}_i\rvert$	MAE	Multimodal distributed data	Convergence problems
			Not to penalize outliers	
Classification	$-\sum_{i=0}^{k} y_i * \log \hat{y}_i$	Category Crossentropy	Multilabel classification	The activation function of output layer must be Softmax
	$-\frac{1}{k}\sum_{i=0}^{k} y_i \text{ x} \log \hat{y}_i + (1 - y_i) \text{ x} \log (1 - \hat{y}_i)$	Binary Crossentropy	Binary classification	The activation function of output layer must be Sigmoid
		Softmax	Binary classification	
Segmentation	$-\frac{1}{k}\sum_{i=0}^{k} y_i \text{ x} \log \hat{y}_i + (1 - y_i) \text{ x} \log (1 - \hat{y}_i)$	Binary Crossentropy	Binary classification	The activation function of output layer must be Sigmoid
	$1 - Dice\ Coefficient$	Dice Loss	Segmentation tasks	

Whereas:

$$Dice\ Coefficient = \frac{2\ x\ |y \cap \hat{y}|}{|y| + |\hat{y}|},$$

Equation 2. 4 - Dice coefficient

$|y \cap \hat{y}|$ is the count of elements that are present in both y (true values) and $\hat{y}$ (predicted values).

$|y|$ is the count of elements in the true values.

$|\hat{y}|$ is the count of elements in the predicted values.

k is the outputs node length.

To conclude, the most important aspect to remember is the selection of the output nodes, the activation, and the loss function, which will depend on the application.

2.4.3. Performance Metrics Functions

To evaluate the performance of models, whether for classification or regression, metrics such as accuracy, precision, recall and F1-score can be considered (Chandrika & Srinivasan, 2021). However, for segmentation, different metrics may be necessary, depending on the difficulty and the complexity of the task. The two most well-known metrics functions for segmentation tasks in the biomedical field are Intersection-over-Union (IoU), also known as Jaccard index, and Dice similarity coefficient (DSC). Both of these metrics are based on the F-score method, where F-score (Müller, D., et al., 2022):

$$F1 = \frac{TP}{TP + \frac{FP + FN}{2}}$$

Equation 2. 5 - F1-Score Equation

Whereas:

TP – True Positive

FP – False Positive

FN – False Negative

The DSC is defined as the harmonic mean between sensitivity and precision. The difference between the two metrics is that the IoU penalizes under- and over-segmentation more than the DSC.

$$IoU = \frac{TP}{TP + FP + FN}$$

Equation 2. 6 **-** Equation of IoU

Besides, both scores are appropriate metrics, the DSC is the most used metric in many publications for segmentation evaluation. DSC equation is demonstrated in the loss equations chapters and in terms of confusion matrix can be calculated as follows:

$$DSC = \frac{2TP}{2TP + FP + FN}$$

Equation 2. 7 **-** DSC Equation

2.4.4. Backpropagation and Optimization Algorithms

Feedforward neural networks take an input x and return an output $\hat{y}$. Information flows forward through the network, with the inputs x providing the initial information that spreads up to the hidden units at each layer and finally generates $\hat{y}$. This process is known as forward propagation.

During training, forward propagation continues until it has a scalar cost, which is generated by the loss function. The backpropagation algorithm enables the flow of information from the cost to compute the gradient for model optimization (Rumelhart et al., 1986). The objective is to determine the optimal weights and bias that minimize the cost.

The figure below (Analytics Vidhya, 2020) presents a simple example of a loss function and its gradient, which is used to adjust the weights. The aim is to identify the minimum point on the curve that corresponds to the weights at which the neural network achieves the highest level of accuracy.

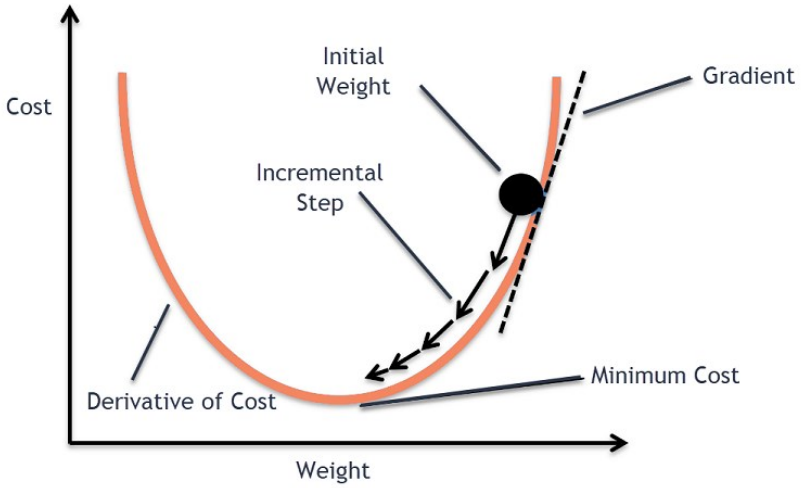

Figure 2. 11 - Gradient Descend Representation-cost function in function of the weights.

Finding the local minimum in this example is a straightforward process. When the slope is negative, the weights should increase, and vice-versa. The exact amount added or subtracted from the weights is referred to as the learning rate. Determining the ideal learning rate can be a challenging task. Values that are too large may overshoot the minimum, while values that are too low will increase training time and may not reach the minimum value within the designated epochs. However, it is unlikely to encounter a graph like this in real-life applications. In such scenarios, the gradient has N-dimensions, each with multiple peaks and valleys. Therefore, the challenge is to identify the global minimum and avoid being misled by nearby local minima.

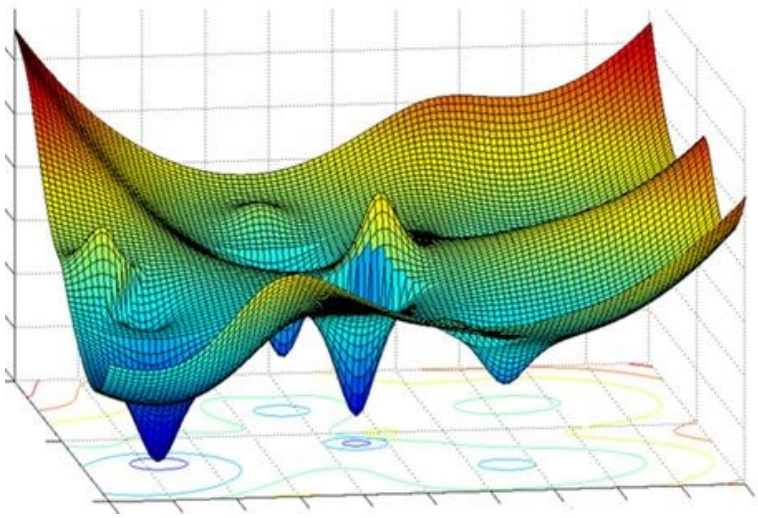

Figure 2. 12 **-** Gradient Descend

The typical method for this situation involves the use of the Stochastic Gradient Descent (SGD) algorithm. The algorithm starts with a set of initial random parameters and updates them incrementally to minimize the cost function. During each iteration, the gradient of the cost function is computed for each parameter. The gradient shows the direction of the steepest ascent, and by moving in the opposite direction, we can determine the direction of the steepest descent. The learning rate determines the size of the step, which controls the algorithm's speed towards the minimum. The process repeats until the cost function converges to a minimum, indicating that the model has reached the optimal set of parameters (Ruder, S., 2016).

2.4.5. Convolutional Neural Networks

Convolutional Neural Networks (CNNs) are a subtype of Artificial Neural Networks (ANNs). Therefore, all the propositions stated in the previous sections remain the same. The only difference between CNNS and the feedforward or recurrent neural networks is the presence of convolutional layers immediately before the fully connected layer.

This location connectivity allows neurons to be connected only to specific regions of the input, known as local connectivity, enabling the capture of spatial hierarchies in data (LeCun et al., 1989).

Moreover, CNNs use shared weights in their convolutional layers. This means that the same filter, defined by a set of weights, is used for each receptive field over the input. This reduces reducing the number of parameters and allows the network to learn patterns irrespective of their location in the input space (LeCun et al., 1989).

Filters or kernels are also a defining characteristic of CNNs. Typically, these are square matrices with smaller dimensions than the layer to which they are applied. The convolution operation involved sliding the kernel to all possible positions on the image, followed by the dot product between the kernel and the image patch (local receptive field), as shown in Figure 2.13 (Haridas, et al., 2020).

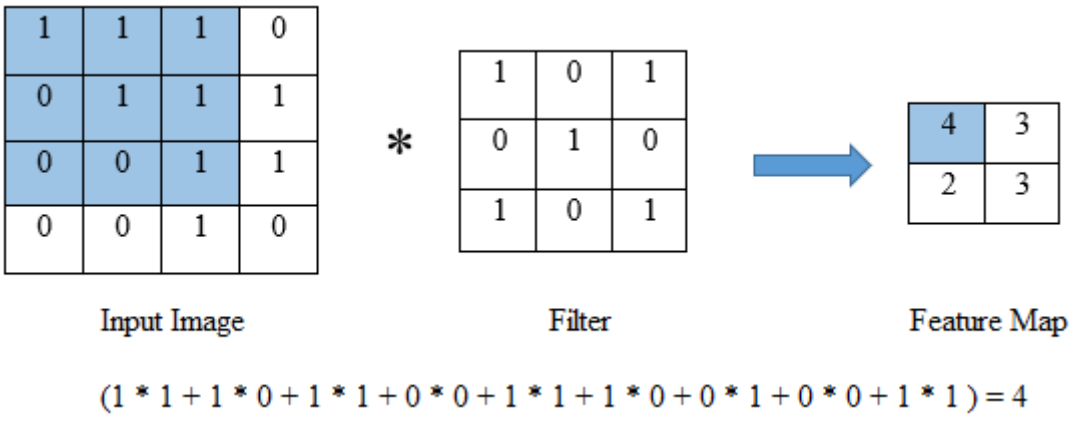

Figure 2. 13 **-** Convolutional Layer process representation, where local receptive field is painted in blue.

In addition, this operation extracts K features from the input image in a single layer, representing distinct features. This leads to K filters and K feature maps. Due to the phenomenon of local receptive field, the number of trainable parameters is significantly reduced. Therefore, it can be considered as a technique for dimensionality reduction.

2.4.5.1. Autoencoder

An autoencoder is a type of CNNs that aims to learn how to reproduce the input image as an output. It consists of an encoder layer, bottleneck, and a decoder layer, as shown in the Figure 2.14. (Bank, Koenigstein, & Giryes, 2021).

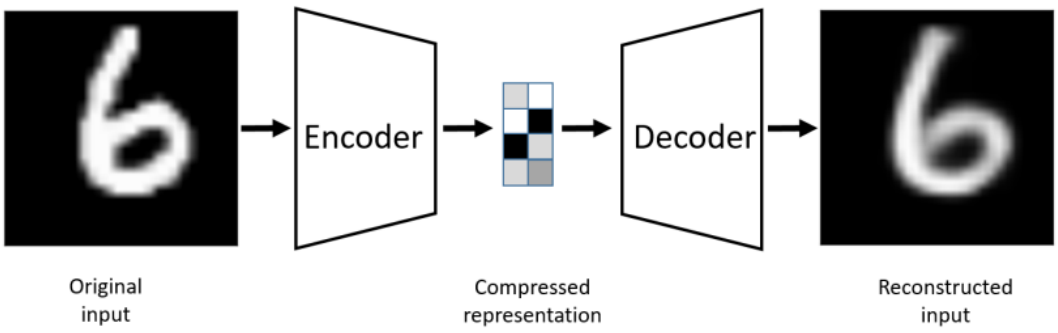

Figure 2. 14 - Autoencoder example, where the original image is compressed and reconstructed (Bank, Koenigstein, & Giryes, 2021)

The encoder component involves reducing the dimensionality of the image using convolution layers until a compressed representation (bottleneck) is obtained. This compressed representation is then used as the starting point for the decoder component. The final part of the network consists of up-sampling layers that reconstruct the original image (Bank, Koenigstein, & Giryes, 2021).

2.4.5.2. U-net Architecture

The U-Net architecture is a subtype of CNNs designed for precise segmentation of biomedical images, even when trained on a limited number of samples. It was originally developed to process medical images where annotations are scarce and costly to obtain. The architecture and training strategy of U-Net, as shown in Figure 2.15, address this challenge (Ronneberger, Fischer, & Brox, 2015).

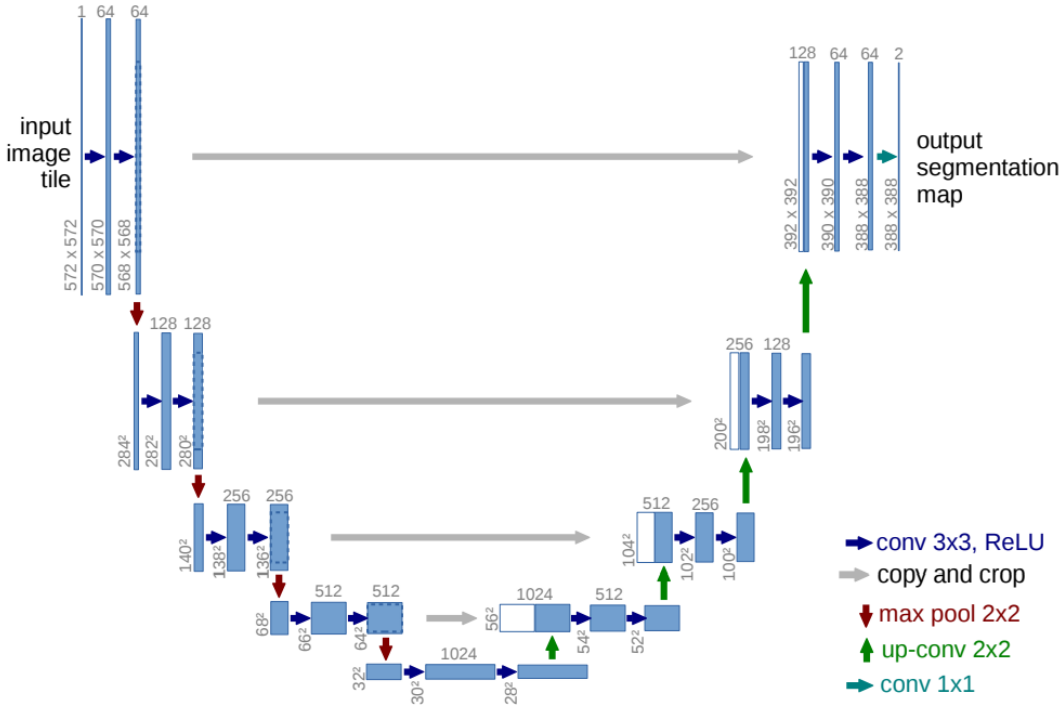

Figure 2. 15 - The U-net architecture, which serves as an example for 32x32pixels in the lowest resolution, is composed of several blue boxes, with each box representing a multi-channel feature map. The number of channels is clearly indicated on top of each box. The dimensions of the box are indicated at the lower left corner. Additionally, white boxes are used to represent copied feature maps, while the arrows depict the various operations being performed.

U-Net architecture is symmetrical with two main paths: the contracting path, which is similar to a conventional CNN, captures the image context through a sequence of

convolutional and max pooling layers. These layers reduce the spatial dimensions while increasing the depth, encapsulating higher-level features at reduced resolutions. This section is responsible for identifying the overall features of the image, such as the existence and approximate location of objects of interest (Ronneberger, Fischer, & Brox, 2015).

The expanding section gradually enhances the spatial dimensions of the processed image through up-convolutions and concatenations with corresponding feature maps from the contracting section. The symmetric expansion in this case allows the network to concentrate on local details and achieve precise localization, which is crucial for accurate segmentation (Ronneberger, Fischer, & Brox, 2015).

2.4.5.3. ResNet

ResNet is a subtype of CNN that resembles U-Net. It is a fully connected layer network that enables the training of extremely deep neural networks. This capability is due to the innovative use of residual blocks, which mitigate the vanishing gradient problem by allowing direct paths for gradient flow through the network architecture. This happens because of the insertion of shortcut connections (He et al., 2015).

ResNets are well-suited for complex image recognition tasks, such as medical image segmentation, where precision is critical for accurate diagnosis and treatment planning.

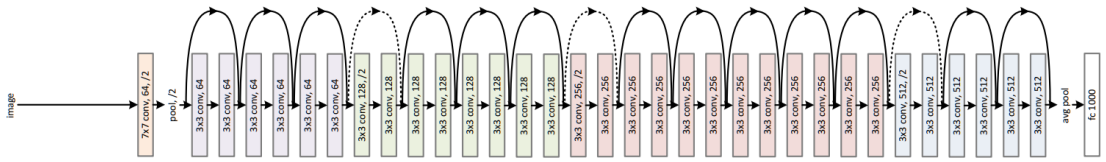

Figure 2. 16 - ResNet architeture example with 34 layers (He et al., 2015)

ResNets can be used to improve the delineation of anatomical structures or pathological regions in medical image segmentation. The deep layers of the architecture can learn rich feature representations, capturing both high-level contextual information and low-level

details necessary for accurate segmentation. Researchers have adapted ResNet architectures for segmentation tasks by incorporating fully convolutional networks (FCNs). This technique replaces fully connected layers with convolutional ones, enabling the network to produce spatial maps instead of classification scores. This combination, known as a ResNet-FCN hybrid, has been shown to significantly improveme the segmentation of medical images with high precision (Long, Shelhamer, & Darrell, 2015; He et al., 2016).

For example, researchers have used a modified ResNet architecture to segment lung nodules from CT scans. This method demonstrated superior performance compared to traditional methods by accurately identifying both large and small nodules (Setio et al., 2016). Additionally, ResNet-based models have been crucial in achieving fine-grained segmentation of different tumor regions in brain tumor segmentation challenges. This has significantly aided in treatment planning and prognosis assessment (Bakas et al., 2018).

2.4.5.4. Transformers

Transformers have revolutionized the way machine learning models comprehend data, surpassing the limitations of previous models that processed data sequentially. This shift is mainly attributed to the novel use of self-attention mechanisms in the architecture, which fundamentally changed the approach to processing sequences (Vaswani et al., 2017).

The Transformer models differs from traditional models in that it uses self-attention to evaluate and assign importance to different segments of the input data relative to each other, regardless of their position. This approach, illustrated in Figure 2.17, enables a dynamic and contextual understanding of the input, thereby improving the model's ability to capture complex dependencies (Vaswani et al., 2017).

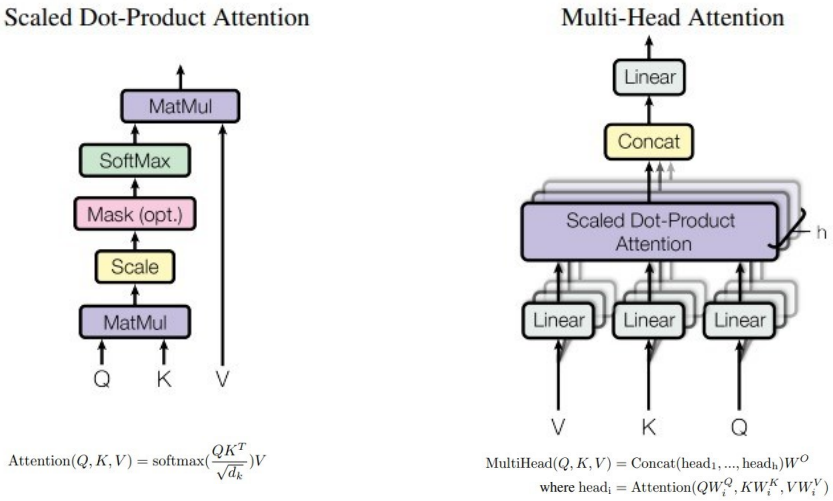

Figure 2. 17 - (left) Scaled Dot-Product Attention. (right) Multi-Head Attention consists of several self-attention heads running simultaneously (Vaswani et al., 2017).

To address the sequential nature of data without relying on sequence-based processing, the Transformer model incorporates positional encoding. This technique provides the input with information about the order of elements, allowing the model to effectively leverage the sequence's positional information (Vaswani et al., 2017).

Figure 2.18 shows the architecture, which is divided into an encoder and decoder, each comprising identical layers. The encoder processes the input using self-attention and feed-forward neural networks to generate a context-aware representation. The output is generated by the decoder iteratively, using its self-attention mechanism to focus on relevant parts of its output. This ensures accurate and contextually relevant predictions (Vaswani et al., 2017).

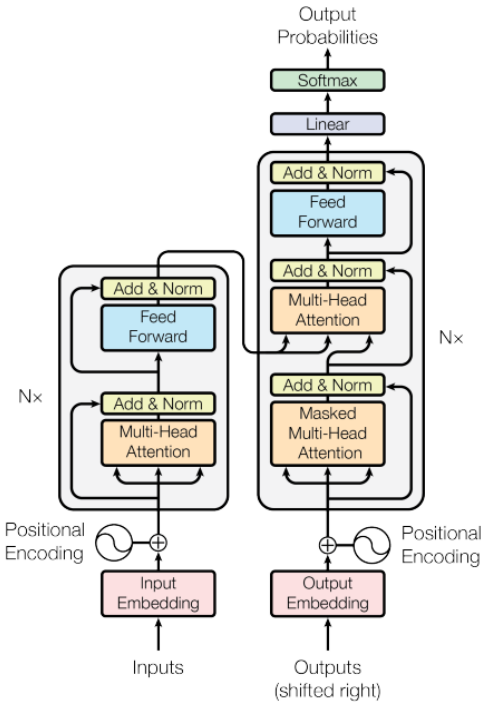

Figure 2. 18 **-** Transformer Architecture (Vaswani et al., 2017).

Recent development in medical imaging included the use of co-encoder models that combine transformer architectures with traditional convolutional networks. These models have been shown to improve feature extraction and segmentation accuracy. Li, Wang, and Li (2022) introduced a transformer and group parallel axial attention co-encoder, which demonstrated improved segmentation performance on various medical imaging tasks. Similarly, in their study, Piao et al. (2023) demonstrated the effectiveness of a HarDNet-based transformer in segmenting intracerebral hemorrhage in CT scan images. The study highlighted the transformer's ability to improve feature learning and segmentation precision.

Transformers have been customized for specific medical segmentation tasks. For example, Wang et al. (2023) used vision transformer adapter-based hyperbolic embeddings to accurately identify and segment multiple lesions in diabetic retinopathy. These models are effective in segmenting complex images and processing them efficiently, making them highly suitable for clinical diagnostics and research.

2.5.MS Lesion Detection in MRI

Accurate detection and segmentation of Multiple Sclerosis lesion in MRI scans is crucial for diagnosing and monitoring the progression of this neurodegenerative disease. Recent advances in deep learning and image processing have resulted in the development of sophisticated algorithms for automated detection and segmentation of MS lesions.

These algorithms can be broadly categorized as patch-wise or semantic-wise segmentation. Patch-wise segmentation uses CNN classifiers and pixel-centered patches for classification, while semantic-wise segmentation employs fully convolutional networks for direct lesion mask prediction. Recent advancements include the use of 3D convolutional networks, feature learning with random forests, and methods for handling missing data modalities. Techniques such as cascade structures and intensity domain adaptation have also been explored to enhance performance and address class imbalance issues. For example, a study by Wahlig et al. (2023), demonstrated that fine-tuning models initially trained on non-MS data with MS-specific data could yield competitive models for identifying existing MS plaques, new MS plaques, and active demyelination with smaller datasets than required for training new models.

Developing algorithms for multiple sclerosis (MS) lesion detection presents several challenges. These include dealing with class imbalance, redundant calculations due to patch overlap in patch-wise segmentation and ensuring robustness against missing input data modalities. Processing time can also be a significant issue, particularly when using complex models and/or handling large datasets. Adapting models to account for intensity variations across different MRI scans also poses a challenge, requiring sophisticated approaches to maintain accuracy and efficiency (Wahlig et al., 2023).

Learning-based algorithms for detecting MS lesions have been improved through the use of synthetic data generation and soft attention mechanisms. These approaches enhance network performance, reduce overfitting, and enable the extraction of lesion locations. The integration of synthetic lesions in training processes has shown significant improvements in identifying cases with lesions (Shmueli et al., 2022).

Another study involved the development of a fully automated method that does not rely on anatomical prior information has been developed. This method is based on an over-segmentation in superpixels and their classification using Gauss-Markov Measure Fields (GMMF), which is robust to noise and computationally efficient (Reyes et al., 2020).

The study employed SynergyNet, a network that utilizes both global and local perspectives to improve segmentation of MS lesions across different sizes. The framework implements local segmentation by augmenting the U-Net architecture with the Mask R-CNN framework (Vang et al., 2020).

A method has been developed to homogenize model results across different datasets and optimize generalization across various sites or scanners. This approach integrates one-shot adaptation data with harmonized training data incorporating labels. It synthesises new training data with contrast similar to the test domain, referred to as "contrast harmonization" in MRI (Zhang et al., 2023).

Additionally, a modified algorithm based on the histone-based fast fuzzy C-means (HFFCM) has been developed for segmenting MS lesions in the white matter of the central nervous system, offering high segmentation accuracies (Bhanumurthy & Anne, 2016).

Table 2.6 summarizes the algorithms mentioned in this section.

Table 2. 6 - Concatenation of MS Lesion detection and Segmentation model's metrics

Study Author(s)	Year	Image Modality	Model/Algorithm	Key Metrics	Highlights
Wahlig et al.	2023	T1 and T1-W	3D U-Net with Transfer Learning	Sensitivity: 0.55; PPV: 0.66	Improved performance with transfer learning; effective with smaller MS-specific datasets.
Shmueli et al.	2022		Deep Learning with Synthetic Data and Soft Attention	Accuracy: 0.91	Utilizes synthetic data and attention mechanisms; reduces overfitting, improves lesion location extraction.
Reyes et al.	2020		Superpixels and Markov Random Fields	DSC:0.7 Sensitivity :0.72	Fully automatic; does not rely on anatomical information; robust to noise.
Vang et al.	2020		SynergyNet: Fusion Framework	Dice Score Improvement: 2.55%; Lesion True Positive Rate: 5.0%	Fuses global and local data perspectives; leverages U-Net and Mask R-CNN framework.
Zhang et al.	2023		Harmonization-enriched Domain Adaptation	DSC: 0.6 F1-Score:0.45	Integrates one-shot adaptation with harmonized training data; effective for domain generalization errors.
Bhanumurthy & Anne	2016		Automated MRI Segmentation Framework	Sensitivity: 0.49 Accuracy:0.96 FNR:0.5	Focuses on segmentation of MS lesions; utilizes histon-based fast fuzzy C-means.

PPV: Positive Predictive Value

DCS:Dice Score Coefficient

FNR: False Negative Rate

The progress made in the detection and segmentation of MS lesions through the use of advanced algorithms is a significant development in the fields of medical imaging and neurology. These algorithms, which utilize deep learning, probabilistic methods, and synthetic data, provide improved accuracy, efficiency, and potential for early diagnosis and monitoring of MS.

3. Materials and Methods

3.1. Dataset

The dataset used for this project was downloaded from the Mendeley website. It is a comprehensive collection of brain MRI data focused on multiple sclerosis (MS), including multi-sequence MRI data from 60 patients diagnosed with MS, along with consensus manual lesion segmentation and detailed patient meta and clinical information. This resource contains T1-weighted, T2-weighted, and fluid-attenuated inversion recovery (FLAIR) MRI sequences that have been meticulously segmented and validated by a team of experienced radiologists and neurologists. It is the most extensive dataset of its kind available to the public and served as a benchmark for automated MS lesion quantification, automated EDSS (Extended Disability Status Scale) prediction and the investigation of correlations between MS lesion characteristics and patient disability. The value of this technology extends to biomedical engineering, medical imaging, and neuroimaging research. It provides a key tool for advances in automated lesion segmentation, disability prediction and the study of MRI brain abnormalities in MS (Muslim, A. M., 2022).

In this study, T2-FLAIR images and their segmentation were isolated and organized by patient for further analysis.

3.2. Hardware and Software

The project was developed on an HP ENVY Laptop - 15-ep0098nr, which includes UHD Graphics and NVIDIA® GeForce RTX™ 2060 with Max-Q design to accelerate model training. All models were developed using the Pytorch lightning framework, in VSCode with python version 3.11.6.

3.3. Image Preprocessing and Augmentation

The integration of deep learning techniques has significantly advanced the field of medical imaging, improving the analysis, interpretation, and prediction capabilities based on medical images. At the core of this integration lies the critical process of medical image

preprocessing, which prepares raw imaging data for further analysis by deep learning models.

Medical image preprocessing involves several techniques aimed at improving image quality. Techniques such as denoising, normalization, histogram equalization and enhancement are crucial for removing artifacts and irrelevant noise from images. Thamilselvan (2022) highlight the importance of denoising in lung cancer images, stating that effective image denoising techniques are necessary for preserving edges while minimizing noise as much as possible. Kebaili, Lapuyade-Lahorgue, and Ruan (2023) investigate the significance of data augmentation in addressing the challenge of limited training data, a common obstacle in medical image analysis. They evaluate deep generative models that generate a variety of realistic training samples, thereby aiding in the effecient training of deep learning models.

The field of medical image analysis has been transformed by deep learning, particularly with the emergence of Convolutional Neural Networks (CNNs) and other neural network architectures. These models have shown remarkable efficacy in tasks such as image classification, segmentation, and anomaly detection. Raad et al. (2021) emphasized the significance of preprocessing in CNN performance for medical image segmentation. The study revealed that the model's performance is highly dependent on the preprocessing steps taken.

Therefore, for this project, several preprocessing steps were implemented. Firstly, skull striping to remove non brain tissue from neuroimage data was performed. Subsequently, image normalization was performed, so pixel values were normalized between 0 and 1 instead of 0 and 255, as grayscale images. The images underwent a Gaussian blur filter was applied to reduce image high-frequency noise and detail, resulting a smoothing effect, that enhanced the structures of interest. Additionally, rotations and flips were also taken into consideration.

The skull stripping process was performed using the FMRIB Software Library, commonly recognized as FSL, which is a collection of tools for analyzing functional magnetic resonance imaging, magnetic resonance imaging and diffusion brain imaging data. The recursive method of Brain Extraction Tool (BET) from FSL was used.

The remaining operations were implemented on the transforms from the Pytorch vision framework.

Furthermore, image augmentation was performed to increase the number of samples, as the number of samples was too small to train a neural network efficiently.

4. Results and Discussion

This section describes the results obtained and provides detailed information on the steps involved in this project.

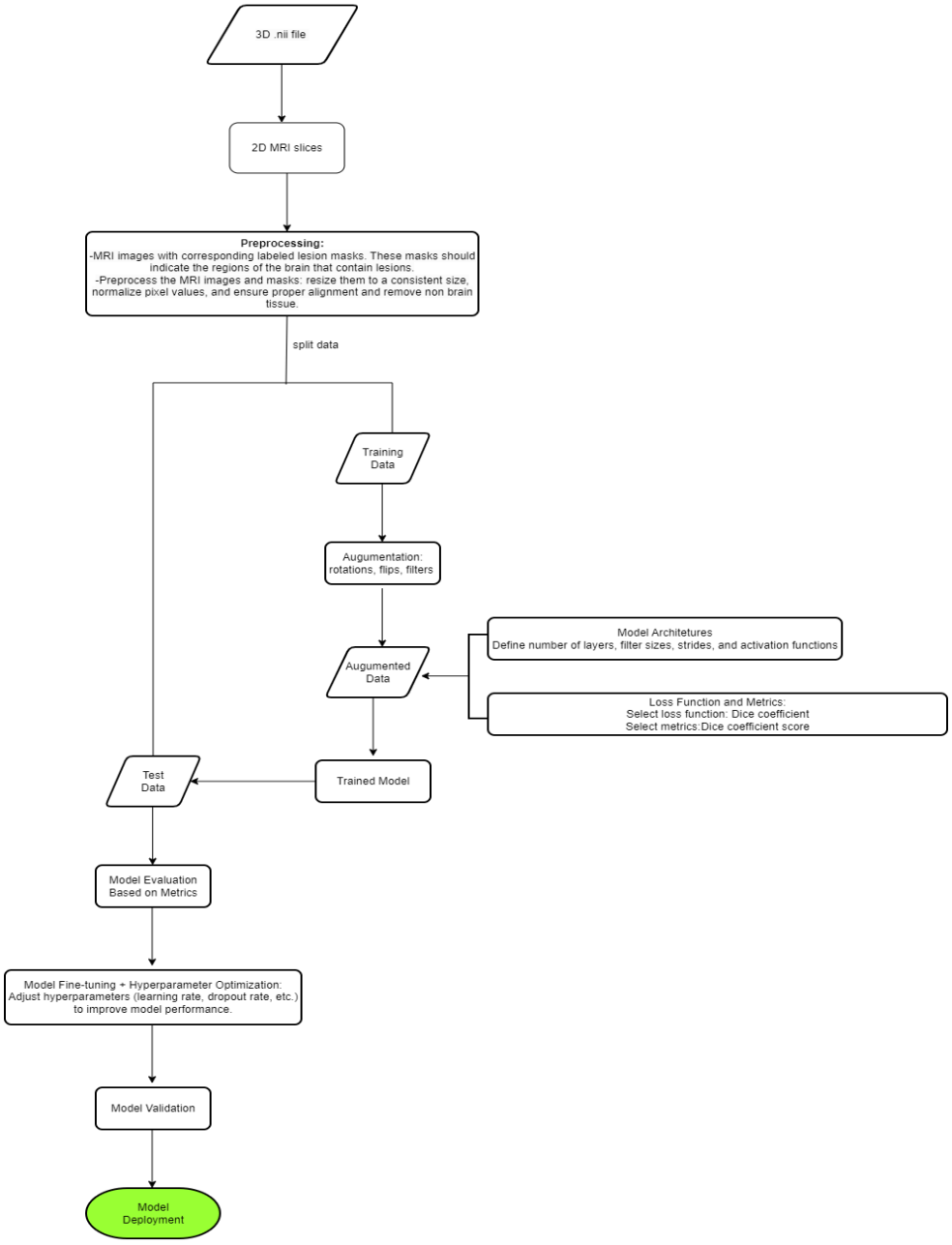

Figure 4. 1 - Project Development Algorithm

The above figure (Figure 4.1.) shows the algorithm for the completion of this project. It starts with uploading and slicing the original .nii files, preprocessing of the images and augmenting both the original and the mask images after the splitting of the data into training and validation. It is also showing the model training steps, namely the choice of

architecture, loss and activation function, model evaluation and model fine-tuning by optimizing the hyperparameters.

Considering that the objective of this study is segmentation, the metrics were defined as Dice Coefficient for model evaluation and Dice Loss as loss function.

Starting from the beginning of the algorithm of the project, the first thing to do is to load the 3D .nii files into the python environment, and unstack them into 2D images, so that each slice of the brain corresponds to a different image and the middle slices were selected (15 per patient). The 3D files were first considered and fed into a 3D Resnet, but as expected, this resulted in immediate overfitting due to the reduced number of patients in the dataset. It was therefore decided that, with the limited resources available, it was to work with 2D images, hence the unstacking part.

In terms of image preprocessing, a simple streamlit application was developed to evaluate the brain extraction method from FSL, BET, to remove the non-brain regions, as shown in Figure 4.2. This method per se does not work perfectly on T2 images, leading to the need for optimization, which was achieved by changing the contrast to resemble T1. Even with the optimization, there were some cases where the extraction was not perfect, i.e., some bone tissue was not removed. Despite this, the extraction can be considered sucessful since only a small number of pixels were not removed.

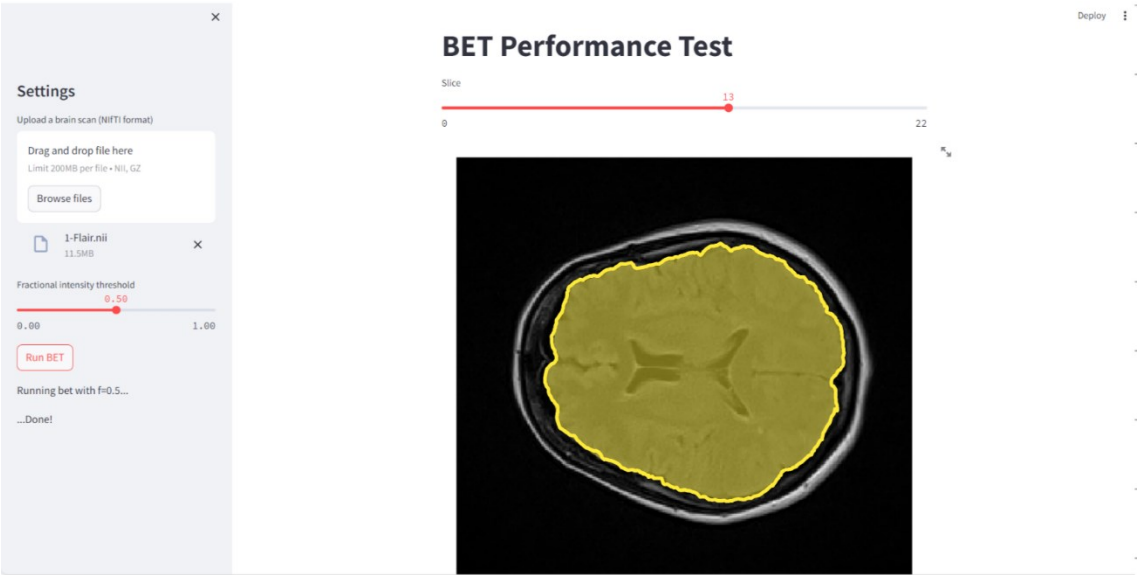

Figure 4. 2 **-** Brain Extraction Tool Visualization

The use of Artificial Neural Networks (ANNs) in medical image segmentation is a crucial development in the application of computational intelligence to enhance clinical diagnosis. ANNs are well-suited to identify complex patterns in high-dimensional data, due to their architecture.

This section outlines the specific architectures and methods employed in this project, including Autoencoders, U-Net, ResNet, and Transformer, to achieve accurate segmentation of MRI images for patients with multiple sclerosis. The order of attempts was established based on the ascending complexity of the networks, allowing the model to detect the patterns while considering the reduced sample size.

The preprocessed dataset was initially divided into training and validation data to enable model evaluation and comparison.

The first attempt at automated lesion segmentation involved using an autoencoder without feeding the ground truth input, meaning, the model attempted to identify the correct features and patterns independently without access to the truth segmentation, resulting in unsupervised learning. The model was constructed with 4 contracting layers and an image input of 224x224. The model achieved a Dice Coefficient of 0.34 on the validation set. As explained on Chapter 2.4.3., the Dice Coefficient is a metric that penalizes under- and over-segmentation. Upon analysis of some outputs, it became apparent that the segmentation of the eye appearance posed a significant challenge. This is illustrated in Figure 4.3.

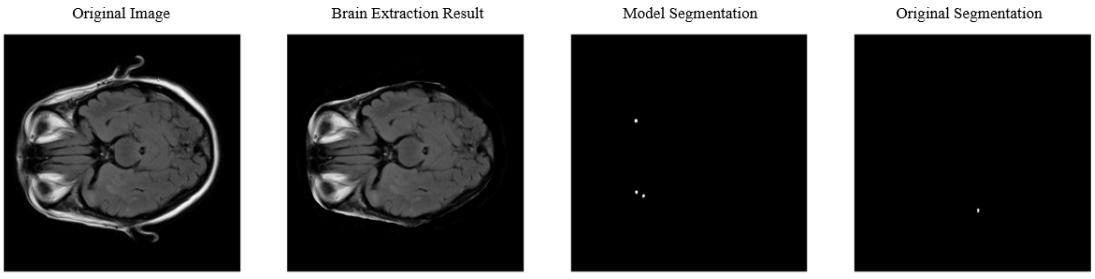

Figure 4. 3 - Typical behavior on this model: eye interference and negligence of the lesion

An autoencoder was also employed, but this time the segmentation images were fed to the model as model outputs. The model architecture, image size, and ground truth presence were the same as the autoencoder mentioned above. The dice coefficient

increased to 0.47, but under-segmentation remained an issue in failed cases, as shown in Figure 4.4. Additionally, eye presence was also a constraint in some cases.

In this particular case, on Figure 4.4, is present also over-segmentation, being the only case this happened on models validation.

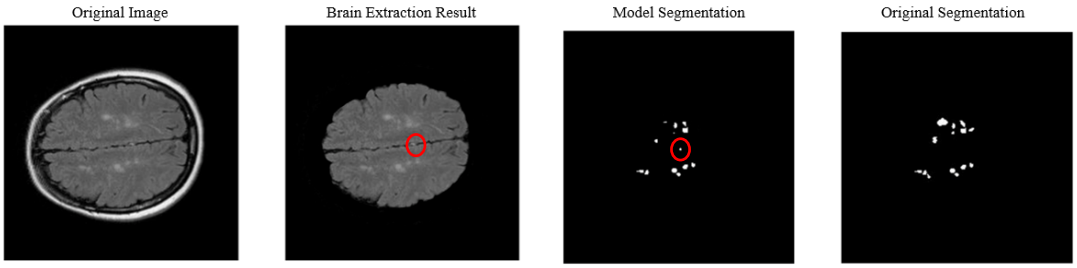

Figure 4. 4 **-** Segmentation Performed by Autoencoder Model with true ground.

Due to unsatisfactory results in the last two attempts, deeper architectures were employed, specifically ResNet and U-Net. The ResNet model was constructed 18 layers and an input size of 224x224. Although this model is typically used for RGB images with 3 channels, it was adapted to work with grayscale images with 1 channel. The dice coefficient improved to 0.53. This suggests that deeper networks may perform better on this type of data.

However, the model discussed here, as well as those that will be discussed further, suffer from under-segmentation.

The U-Net model, a popular model for brain MRI from Pytorch hub, served as the base architecture for this task. Originally developed to detect abnormalities in brain volumes (Mateusz Buda, 2019), this model is similar to ResNet model and is designed to receive three channel images as input. It has been adapted to accept one channel images and an input size of 224x224. This model has 24 layer and achieved a dice coefficient of 0.56, which is similar to the ResNet model.

Finally, to test one of the most recent and powerful architectures available, a visual transformer was implemented. This specific architecture provides the possibility of having spatial context and attention to the surrounding tissue, which can be beneficial for this task. The model was designed to accept 224x224 images as input with a kernel size (token) of 16x16 patches, based on the ViT model from Google (Google AI, 2020), and

with 12 layers of attention. The model achieved the highest dice coefficient of 0.58, among the models discussed, as Figure 4.5 shows. This is a positive indication, although it was not expected to perform flawlessly due to the limited dataset size. As the network becomes deeper, the risk of overfitting increases, making it crucial to have large number of samples (Gygi, Kleinstein, & Guan, 2023).

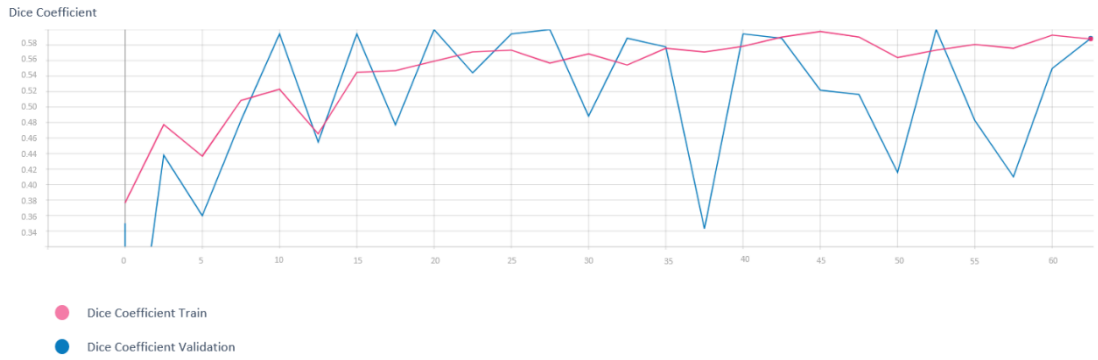

Figure 4. 5 **-** Model metrics in train and validation set

During the construction of these models, hyperparameter tuning was performed using Optuna (Optuna, 2019), a python package that enables hyperparameter tuning by defining the objective function and interactively calculating the model to obtain the best results. The results presented in this section are the best achieved. The table below shows a compilation of the results obtained.

Table 4. 1 - Model's results compilation

Model Type	**Segmentation**	**Dice Coefficient in validation**	**Dice Loss in validation**
Autoencoder	No	0.34	0.66
Autoencoder	Yes	0.47	0.53
ResNet	Yes	0.53	0.47
U-Net	Yes	0.56	0.44
Visual Transformer	Yes	0.58	0.42

5. Conclusions

To achieve the objective of this project, i.e. to develop a model capable of performing automatic segmentation of Multiple Sclerosis lesions on the 2D T2-FLAIR modality using artificial intelligence, several steps were considered to have been carried out, namely image pre-processing and augmentation, model definition, hyperparameter tunning and finally model evaluation.

Regarding the first part of the steps, image pre-processing and augmentation, including brain isolation were considered to be successfully completed, although in some cases some bone tissue was not completely removed, as the methods were originally developed to be performed on other magnetic resonance imaging modalities. However, in the vast majority of cases it worked very well.

The study of the application of Artificial Neural Networks (ANNs) to the segmentation of MRI images in patients with Multiple Sclerosis has provided important insights. Starting with an unsupervised autoencoder, it was possible to identify the limitations in the segmentation accuracy, as evidenced by the initial Dice Coefficient. Incorporating ground truth into the autoencoder model improved performance, but under- and over-segmentation remained a challenge. The use of more sophisticated architectures such as ResNet and U-Net, albeit adapted for greyscale imaging, led to further improvements. However, it was the implementation of the Visual Transformer architecture that marked a leap forward, achieving the highest Dice Coefficient, of almost 60%. This progress illustrates the potential for transformers in medical imaging and confirms the hypothesis that deeper, more complex networks can yield better segmentation results. The deeper as the networks are, the greater the risk of overfitting, so it is reasonable to conclude that this model could have produced better results with more samples.

In conclusion, given the promising advances in the use of Visual Transformers for Multiple Sclerosis lesion segmentation in T2-FLAIR MRI images, which have demonstrated significant improvements in segmentation accuracy and underscored the efficacy of complex neural network architectures, this project not only demonstrates the potential of artificial intelligence to enhance medical imaging analysis, but also represents a fundamental step towards revolutionizing diagnostic methodologies for neurodegenerative inflammatory diseases such as Multiple Sclerosis.

6. Future work

The research carried out in this thesis has shown the possibility of having an automatic lesion segmentation of Multiple Sclerosis on T2 Flair images, although not with the highest score of segmentation that could be achieved. Nevertheless, and with the vision of obtaining better segmentation, it is highly recommended to collect more samples on the one hand, and on the other hand to generate more images through GANs (Generative Artificial Networks), because the more samples the model gets, the more it can learn from them and the deeper the model can be.

Then retrain the model with the new images and their segmentation until the model has the desired performance, continue to feed it with images and establish a design of operations that allows self-learning, i.e., add the samples where the segmentation task of the model is satisfactory to the core dataset of the model and train it again to improve the execution.

Create an infrastructure, where the images and the model are stored, connected to a visualizer capable of ingesting samples and retrieving the segmentation in real time, linked to the operation of self-learning.

Thus, if these steps are successfully carried out, we can affirm that we are in the presence of an expert system, where the artificial intelligence leads the way.

References

Abdelmonem, H. (n.d.). Multiple sclerosis - Dawson fingers. Radiopaedia.org. Retrieved January 14, 2024, from https://doi.org/10.53347/rID-59113

Aggarwal, C. C. (2018) ‘An introduction to neural networks‘, in Aggarwal, C. C. (1sted.) Neural networks and deep learning: A textbook. New York: Springer International Publishing, pp. 1-52.

Analytics Vidhya. (2020). How Does the Gradient Descent Algorithm Work in Machine Learning? Retrieved from https://www.analyticsvidhya.com/blog/2020/10/how-does-the-gradient-descent-algorithm-work-in-machine-learning/

Asadollahzadeh, E., Ghadiri, F., Ebadi, Z., & Moghadasi, A. N. (2023). The correlation of conventional and advanced MRI findings with cognitive function in multiple sclerosis: A systematic review and meta-analysis. Link: Journal of Research in Clinical Medicine.

Available at: https://learn.microsoft.com/en-us/archive/msdn-magazine/2019/a

Avila, M., Okai, A., & DeToledo, J. C. (2017). Chapter 16.2 - Translational Correlation: Multiple Sclerosis. In P. M. Conn (Ed.), Conn's Translational Neuroscience (pp. 359-361). Academic Press. https://doi.org/10.1016/B978-0-12-802381-5.00028-2.

Azhar, S., & Chong, L. (2022). Clinician’s guide to the basic principles of MRI. Link: Postgraduate Medical Journal.

Bakas, S., Akbari, H., Sotiras, A., Bilello, M., Rozycki, M., Kirby, J., Freymann, J.B., Farahani, K., & Davatzikos, C. (2018). Advancing The Cancer Genome Atlas glioma MRI collections with expert segmentation labels and radiomic features. *Nature Scientific Data, 4*, 170117. https://doi.org/10.1038/sdata.2017.117

Bank, D., Koenigstein, N., & Giryes, R. (2021). Autoencoders. arXiv:2003.05991v2 [cs.LG]. https://doi.org/10.48550/arXiv.2003.05991

Barkhof F, van Walderveen M. Characterization of tissue damage in multiple sclerosis by nuclear magnetic resonance. Philos Trans R Soc Lond B Biol Sci. 1999;354(1390):1675–1686.

Bhanumurthy, M., & Anne, K. (2016). An automated MRI segmentation framework for brains with tumors and multiple sclerosis lesions. Link: International Conference on Computation of Power, Energy, Information and Communication.

Brown, R.W., Cheng, Y.N., Haacke, E.M., Thompson, M., & Venkatesan, R. (1999). Magnetic Resonance Imaging: Physical Principles and Sequence Design.

Bueno, A., Bosch, I., Rodríguez, A., et al. (2022). Automated Cervical Spinal Cord Segmentation in Real-World MRI of Multiple Sclerosis Patients by Optimized Hybrid Residual Attention-Aware Convolutional Neural Networks. Link: Journal of Digital Imaging.

Chandrika, P & Srinivasan, Sakthi & Taylor, George. (2021). Predicting Stock Market Movements Using Artificial Neural Networks. Universal Journal of Accounting and Finance. 9. 405-410. 10.13189/ujaf.2021.090315.

Compston, A., & Coles, A. (2008). Multiple Sclerosis. Lancet, 372(9648), 1502–1517.

Costa, V. G. C., Alves-Leon, S. V., & Gomes, F. C. A. (2023). Central nervous system demyelinating diseases: glial cells at the hub of pathology. Frontiers in Immunology, 14. Link: https://doi.org/10.3389/fimmu.2023.1135540

Dasgupta, Somsankar & Ray, Swapan. (2019). Ceramide and Sphingosine Regulation of Myelinogenesis: Targeting Serine Palmitoyltransferase Using microRNA in Multiple Sclerosis. International Journal of Molecular Sciences. 20. 5031. 10.3390/ijms20205031.

Dobson R, Giovannoni G. Multiple sclerosis - a review. Eur J Neurol. 2019 Jan;26(1):27-40. doi: 10.1111/ene.13819. Epub 2018 Nov 18. PMID: 30300457.

Durstewitz, Daniel & Koppe, Georgia & Meyer-Lindenberg, Andreas. (2019). Deep neural networks in psychiatry. Molecular Psychiatry. 24. 1. 10.1038/s41380-019-0365-9.

Filippi, M., Brück, W., Chard, D., et al. (2019). Association between pathological and MRI findings in multiple sclerosis.

Filippi, M., Rocca, M., Barkhof, F., et al. (2012). Association between pathological and MRI findings in multiple sclerosis.

FMRIB Analysis Group. (2024). FSL. Retrieved from https://fsl.fmrib.ox.ac.uk/fsl/fslwiki

Foschi, M., Rizzo, G., Liguori, R., et al. (2019). Sleep-related disorders and their relationship with MRI findings in multiple sclerosis. Link: Sleep Medicine.

Ghasemi, N., Razavi, S., & Nikzad, E. (2017). Multiple Sclerosis: Pathogenesis, Symptoms, Diagnoses and Cell-Based Therapy. Cell journal, 19(1), 1–10. https://doi.org/10.22074/cellj.2016.4867

Goodfellow, I., Bengio, Y., Courville, A. (2016) Deeplearningbook. MIT Press.

Google AI. (2020). ViT-Base-Patch16-224. Hugging Face. Retrieved February 12, 2024, from https://huggingface.co/google/vit-base-patch16-224

Graupe, D. (2013) Advanced Series in Circuits and Systems. Singapore: World Scientific.

Gygi, J. P., Kleinstein, S. H., & Guan, L. (2023). Predictive overfitting in immunological applications: Pitfalls and solutions. *Human vaccines & immunotherapeutics*, *19*(2), 2251830. https://doi.org/10.1080/21645515.2023.2251830

Habibi Aghdam, H., Jahani Heravi, E. (2017). Convolutional Neural Networks. In: Guide to Convolutional Neural Networks. Springer, Cham. https://doi.org/10.1007/978-3-319-57550-6_3

Hadican. (2019). How to Build a Simple Artificial Neural Network (ANN). Medium. Side-by-side illustrations of biological and artificial neurons. How to Build a Simple Artificial Neural Network (ANN) | by hadican | Medium)

Haridas, Arjun & Dyrba, Martin. (2020). Comparison of Convolutional neural network training parameters for detecting Alzheimers disease and effect on visualization.

Hauw, J.-J., Delaére, P., Seilhean, D., & Cornu, P. (1992). Morphology of demyelination in the human central nervous system. Journal of Neuroimmunology, 40(2–3), 139-152. https://doi.org/10.1016/0165-5728(92)90128-8.

He, K., Zhang, X., Ren, S., & Sun, J. (2015). Deep Residual Learning for Image Recognition. arXiv:1512.03385. Retrieved from https://arxiv.org/pdf/1512.03385.pdf

He, K., Zhang, X., Ren, S., & Sun, J. (2016). Deep Residual Learning for Image Recognition. *Proceedings of the IEEE Conference on Computer Vision and Pattern Recognition (CVPR)*, 770-778. https://doi.org/10.1109/CVPR.2016.90

Jadon, S. (2020). A survey of loss functions for semantic segmentation. 2020 IEEE Conference on Computational Intelligence in Bioinformatics and Computational Biology (CIBCB), 1-7.

Kebaili, A., Lapuyade-Lahorgue, J., & Ruan, S. (2023). Deep Learning Approaches for Data Augmentation in Medical Imaging: A Review.

Kuhlmann, T., & Antel, J. (2023). Multiple sclerosis: 2023 update. Free Neuropathology, 4, Article 4-3. https://doi.org/10.17879/freeneuropathology-2023-4675.

Kwok, W. (2022). Basic Principles of and Practical Guide to Clinical MRI Radiofrequency Coils. Link: Radiographics.

Lamb YN. Ocrelizumab: A Review in Multiple Sclerosis. Drugs. 2022 Feb;82(3):323-334. doi: 10.1007/s40265-022-01672-9. Epub 2022 Feb 22. PMID: 35192158; PMCID: PMC8862399.

LeCun, Y., Boser, B., Denker, J. S., Henderson, D., Howard, R. E., Hubbard, W., & Jackel, L. D. (1989). Backpropagation applied to handwritten zip code recognition. Neural Computation, 1(4), 541-551.

Li, C., Wang, L., & Li, Y. (2022). Transformer and group parallel axial attention co-encoder for medical image segmentation. Scientific Reports. https://www.nature.com/articles/s41598-022-20440-z.pdf

Liu, J., Wang, Y., Katscher, U., & He, B. (2017). Electrical Properties Tomography Based on B1 Maps in MRI: Principles, Applications and Challenges. Link: IEEE Transactions on Biomedical Engineering.

Long, J., Shelhamer, E., & Darrell, T. (2015). Fully Convolutional Networks for Semantic Segmentation. *Proceedings of the IEEE Conference on Computer Vision and Pattern Recognition (CVPR)*, 3431-3440. https://doi.org/10.1109/CVPR.2015.7298965

Lopaisankrit, T., & Thammaroj, J. (2023). Brain and Spinal Cord MRI Findings in Thai Multiple Sclerosis Patients. Link: Journal of Imaging.

Mateusz Buda. (2019). U-Net for brain MRI. PyTorch Hub. Retrieved January 25, 2024, from https://pytorch.org/hub/mateuszbuda_brain-segmentation-pytorch_unet/

McCulloch, W. S., & Pitts, W. (1943). A logical calculus of the ideas immanent in nervous activity. University of Illinois, College of Medicine, Department of Psychiatry at the Illinois Neuropsychiatric Institute, and the University of Chicago

Meca-Lallana, V., Berenguer-Ruiz, L., Carreres-Polo, J., Eichau-Madueño, S., Ferrer-Lozano, J., Forero, L., Higueras, Y., Téllez Lara, N., Vidal-Jordana, A., & Pérez-Miralles, F. C. (2021). Deciphering Multiple Sclerosis Progression. Frontiers in Neurology, 12. https://doi.org/10.3389/fneur.2021.608491

Miller, K., Alfaro-Almagro, F., Bangerter, N., et al. (2016). Multimodal Population Brain Imaging in the UK Biobank Prospective Epidemiological Study. Link: Nature Neuroscience.

Müller, D., Soto-Rey, I., & Kramer, F. (2022). Towards a guideline for evaluation metrics in medical image segmentation. BMC research notes, 15(1), 210. https://doi.org/10.1186/s13104-022-06096-y

Multiple Sclerosis International Federation. Atlas of MS 2013, mapping the multiple sclerosis over the world; 2013

Muslim, A. M., Mashohor, S., Gawwam, G. A., Mahmud, R., Hanafi, M. binti, Alnuaimi, O., Josephine, R., Almutairi, A. D. (2022). Brain MRI dataset of multiple sclerosis with consensus manual lesion segmentation and patient meta information. Data in Brief, 42.

National Institute of Neurological Disorders and Stroke. (n.d.). Multiple Sclerosis. Retrieved from https://www.ninds.nih.gov/health-information/disorders/multiple-sclerosis

National Multiple Sclerosis Society. (2023). Secondary progressive MS. National Multiple Sclerosis Society. Retrieved from https://www.nationalmssociety.org/What-is-MS/Types-of-MS/Secondary-progressive-MS

Optuna. (2019). Key Features. Retrieved December 15, 2023, from Optuna - A hyperparameter optimization framework

Pekel, E., & Kara, S. S. (2017) 'A comprehensive review for artifical neural network application to public transportation'. Sigma Journal of Engineering and Natural Sciences, 35(1), 157-179.

Piao, Z., Gu, Y. H., Jin, H., & Yoo, S. J. (2023). Intracerebral hemorrhage CT scan image segmentation with HarDNet based transformer. Scientific Reports. https://www.nature.com/articles/s41598-023-33775-y.pdf

Raad, K. B. D., van Garderen, K. A., Smits, M., Voort, S. V. D., Incekara, F., Oei, E., Hirvasniemi, J., Klein, S., & Starmans, M. P. (2021). The Effect of Preprocessing on Convolutional Neural Networks for Medical Image Segmentation.

Raschka, S. (2016). Activation Functions in Neural Networks. Retrieved from https://sebastianraschka.com/faq/docs/activation-functions.html

Reyes, A., Alba, A., Méndez, M., et al. (2020). Probabilistic Multiple Sclerosis Lesion Detection using Superpixels and Markov Random Fields. Link: Semanticscholar.

Ronneberger, O., Fischer, P., & Brox, T. (2015). U-Net: Convolutional Networks for Biomedical Image Segmentation. arXiv:1505.04597. https://arxiv.org/abs/1505.04597

Ruder, S. (2016). An overview of gradient descent optimization algorithms. ArXiv.

Rumelhart, D.E., Hinton, G.E. and Williams, R.J. (1986) 'Learning representations by back-propagating errors', Nature, 323(6088), pp. 533–536. Available at: https://doi.org/10.1038/323533a0

Sahraian MA, Radue EW, Haller S, Kappos L. Black holes in multiple sclerosis: definition, evolution, and clinical correlations. Acta Neurol Scand. 2010;122(1):1–8.

Setio, A. A. A., Traverso, A., de Bel, T., Berens, M. S. N., van den Bogaard, C., Cerello, P., Chen, H., Dou, Q., Fantacci, M. E., Geurts, B., van der Gugten, R., Heng, P. A., Jansen, B., de Kaste, M. M. J., Kotov, V., Lin, J. Y. H., Manders, J. T. M. C., Sánchez, C. I., Schaap, M., Silva, C. A., Snoeren, M., Prokop, M., Smitsmans, M. H. P., Tang, H., Tarando, S., de Wee, J. A., van Wijk, C., Yung, W. N., Zhao, J., & Zhao, Y. (2016). Validation, comparison, and combination of algorithms for automatic detection of pulmonary nodules in computed tomography images: The LUNA16 challenge. *Medical Image Analysis, 42*, 1-13. https://doi.org/10.1016/j.media.2017.06.015

Shah, K., & Abbruscato, T. (2017). Chapter 6 - The Blood–Brain Barrier: A Restricted Gateway to the Brain. In P. M. Conn (Ed.), Conn's Translational Neuroscience (pp. 141-146). Academic Press. https://doi.org/10.1016/B978-0-12-802381-5.00010-5

Shmueli, O., Solomon, C., Ben-Eliezer, N., & Greenspan, H. (2022). Deep learning-based multiple sclerosis lesion detection utilizing synthetic data generation and soft attention mechanism. Link: Semanticscholar.

Suzuki, K. (2013) Artificial neural networks - Architectures and applications. Rijeka,

Thamilselvan, P. (2022). IMPROVING MEDICAL IMAGE PREPROCESSING USING DENOISING TECHNIQUE.

Thau, L., Reddy, V., & Singh, P. (2022). Anatomy, Central Nervous System. In StatPearls. Treasure Island (FL): StatPearls Publishing. Retrieved from https://www.ncbi.nlm.nih.gov/books/NBK542179/.

Thompson AJ, Banwell BL, Barkhof F, Carroll WM, Coetzee T, Comi G, Correale J, Fazekas F, Filippi M, Freedman MS, Fujihara K, Galetta SL, Hartung HP, Kappos L, Lublin FD, Marrie RA, Miller AE, Miller DH, Montalban X, Mowry EM, Sorensen PS, Tintoré M, Traboulsee AL, Trojano M, Uitdehaag BMJ, Vukusic S, Waubant E, Weinshenker BG, Reingold SC, Cohen JA. Diagnosis of multiple sclerosis: 2017 revisions of the McDonald criteria. Lancet Neurol. 2018 Feb;17(2):162-173. doi: 10.1016/S1474-4422(17)30470-2. Epub 2017 Dec 21. PMID: 29275977.

Tortora G, Derrickson B. Principles of Anatomy & Physiology. 13th ed. Johan Wiley & Sons; 2011.

Vandergriendt, C., Zimlich, R., (2022). An Easy Guide to Neuron Anatomy with Diagrams. Healthline. Retrieved from https://www.healthline.com/health/neurons#takeaway

Vang, Y. S., Cao, Y., Chang, P., et al. (2020). SynergyNet: A Fusion Framework for Multiple Sclerosis Brain MRI Segmentation with Local Refinement. Link: IEEE International Symposium on Biomedical Imaging.

Vaswani, A., Shazeer, N., Parmar, N., Uszkoreit, J., Jones, L., Gomez, A. N., Kaiser, Ł., & Polosukhin, I. (2017). Attention is all you need. In Advances in Neural Information Processing Systems (pp. 5998-6008).

Wahlig, S. G., Nedelec, P., Weiss, D., et al. (2023). 3D U-Net for automated detection of multiple sclerosis lesions: utility of transfer learning from other pathologies. Link: Frontiers in Neuroscience.

Walton, C., King, R., Rechtman, L., et al. (2020). Rising prevalence of multiple sclerosis worldwide: Insights from the Atlas of MS, third edition. Multiple Sclerosis Journal, 26(14), 1816-1821. https://doi.org/10.1177/1352458520970841

Walton, C., King, R., Rechtman, L., Kaye, W., Leray, E., Marrie, R. A., Robertson, N., La Rocca, N., Uitdehaag, B., van der Mei, I., Wallin, M., Helme, A., Angood Napier, C., Rijke, N., & Baneke, P. (2020). Rising prevalence of multiple sclerosis worldwide: Insights from the Atlas of MS, third edition. *Multiple sclerosis (Houndmills, Basingstoke, England)*, *26*(14), 1816–1821. https://doi.org/10.1177/1352458520970841

Wang, Z., Lu, H., Yan, H., Kan, H., & Jin, L. (2023). Vison transformer adapter-based hyperbolic embeddings for multi-lesion segmentation in diabetic retinopathy. Scientific Reports. https://www.nature.com/articles/s41598-023-38320-5.pdf

Warren S. McCulloch and Walter Pitts titled "A Logical Calculus of the Ideas Immanent in Nervous Activity" in the Bulletin of Mathematical Biophysics, Volume 5, from 1943

Wiesinger, F., & Ho, Mai-Lan. (2022). Zero-TE MRI: principles and applications in the head and neck. Link: The British Journal of Radiology.

Wingerchuk, D. M. (2012). Smoking: effects on multiple sclerosis susceptibility and disease progression. Therapeutic Advances in Neurological Disorders, 5(1), 13–22.

World Health Organization. (2023). Multiple sclerosis (MS). WHO. Retrieved December 14, 2023, from https://www.who.int/news-room/fact-sheets/detail/multiple-sclerosis

Zhang, J., Zuo, L., Dewey, B., et al. (2023). Harmonization-enriched domain adaptation with light fine-tuning for multiple sclerosis lesion segmentation. Link: 2310.20586.pdf (arxiv.org)